Investigating Protein Kinase CK2 inhibition in BRAF colon cancer

Benjamin Brown

Department of Chemistry and Biomolecular Sciences,
Macquarie University

A thesis in partial fulfillment of the Master of Research degree

Supervisor: *Associate Professor Mark Molloy*

9th of October 2015

Abstract:

Within colon cancer, the BRAF mutation is a biomarker of poor prognosis, with patients experiencing a median survival of 10 months once the disease has metastasized. These patients are unresponsive to single-agent BRAF inhibition, despite its efficacy in a range of other BRAF cancer types. Recently, phosphosubstrates of protein kinase CK2 were shown to be up-regulated in response to BRAF inhibition in BRAF thyroid cancer. We investigated the efficacy of combined BRAF/protein kinase CK2 inhibition in various BRAF colon cancer cell lines. Dual administration of CX-4945 (CK2i) with Dabrafenib (BRAFi) was effective in reducing cell viability, although not as impressively as previously reported in melanoma and thyroid cancer. Using a label-free phosphoproteomics workflow, a total of 29 phosphopeptides were up-regulated in response to BRAF inhibition. Kinase enrichment analysis of these phosphopeptides revealed that there was no enrichment of protein kinase CK2 substrates. Rather, 58% of the enriched kinases functioned downstream of EGFR. This finding points to the clear need to control EGFR signaling in BRAF colon cancer. Kinase enrichment analysis also revealed that SRC kinase activity was enriched 7.67-fold in response to GDC0941 (PI3Ki), providing rationale for the evaluation of dual PI3K/SRC kinase inhibition in BRAF colon cancer cells.

Declaration

The content of this thesis is original and does not contain material written by another individual, unless a reference to another work has been cited. Effort has also been taken to acknowledge the contribution of others to this work.

Benjamin Brown

Acknowledgements

Firstly, I would like to thank my supervisor, Associate Professor Mark Molloy for his continued guidance and patience throughout the year. I am thankful for his weekly assistance and for the useful feedback provided during the project.

I am also thankful to everyone in the Molloy research group. I am grateful for their ongoing support and help in many areas of the project. I am especially thankful for the mentoring I received from DR. Juan Martinez-Aguilar in areas such as cell culture and phosphopeptide enrichment. I am also especially thankful to DR. Albert Lee for his advice on a range of techniques such as Western blotting and for his assistance with the mass spectrometry experiments. I appreciate the opportunity to have worked in the CBMS and APAF laboratories, as they provided an enjoyable and comfortable working environment.

Finally, I would like to thank my family and friends for their continued support throughout the year. I am especially grateful to my father Vaughan, who ignited my passion for science at an early age. He inspired me to pursue science and has continued to encourage me throughout this year.

Table of Contents

List of Tables

List of Figures

This thesis has been presented in the style of *Proteomics*

Abbreviations

ACN Acetonitrile
APC Adenomatous polyposis coli
AGC Automatic gain control
BSA Bovine serum albumin
DMEM Dulbecco's modified Eagle's medium
EGFR Epidermal growth factor receptor
ERK Extracellular-signal-related kinase
FBS Fetal bovine serum
FDA US Food and Drug Administration
FDR False discovery rate
GPCR G-protein-coupled receptor
IMAC Immobilised metal affinity chromatography
iTRAQ Isobaric tag for relative and absolute quantitation
LFQ Label free quantitation
MAPK Mitogen-activated protein kinase
MOAC Metal oxide affinity chromatography
MS Mass spectrometry
PBS Phosphate buffered saline
PIGF Placental growth factor
PTEN Phosphatase and tensin homolog
RTK Receptor tyrosine kinase
SCX String cation-exchange
SILAC Stable isotope labeling by amino acids in cell culture
TFA Trifluoroacetic acid
VEGF Vascular endothelial growth factor

Introduction:

1.1 Colon cancer

Colon cancer is the third most common cause of cancer worldwide, with an expected 1.2 million new cases each year; 17,000 in Australia alone[1,2]. The five year survival rate for localized colon cancer is >90% but this rapidly declines to approximately 10% in metastatic disease[3]. Whilst screening practices such as colonoscopies improve early detection and thus allow for curative surgery, roughly one in three patients is diagnosed with metastatic disease[4]. Patients with untreated metastatic colon cancer have a survival rate of 6 months, although this can be extended to over 2 years with current treatment regimes.[4]

The backbone of current treatment is 5-fluorouracil, which has been used in combination with a range of other FDA approved agents to extend patient survival[4] (Table 1). The improvement in patient survival from combination therapies can be seen in the recent phase III FIRE-3 clinical trial[5]. Here, the chemotherapy combination FOLFIRI (leucovorin, 5-fluorouracil, and irinotecan) was combined with cetuximab and this resulted in a response rate (as determined by either partial or complete tumor regression) of 72.2% and an overall survival of 28.7 months in colon cancer patients. In contrast, treatment with 5-fluorouracil as a single agent, resulted in a response rate of 31% and an overall survival of 14.1 months[6]. Whilst combinations of cytotoxic agents and biologics have more than doubled the survival rate of metastatic colon cancer patients in the last 20 years, the benefits have not extended to all subtypes of the disease.

Colon cancer can be subdivided based on its B-Rapidly Accelerated Fibrosarcoma protein (BRAF) mutational status. The 85% of patients with wild-type BRAF follow a characteristic disease progression sequence described by the Kinzler-vogelstein model[7]. Here, disease progresses via an adenoma-carcinoma sequence that begins with an initiating loss-of-function mutation in the Adenomatous polyposis coli protein (APC), followed by mutations in tumor protein p53 (p53), v-Ki-ras2 Kirsten rat sarcoma viral oncogene homolog protein (KRAS) and various Wnt signaling pathway proteins. The remaining 15% of patients have an oncogenic gain-of-function mutation in the BRAF protein[8]. This molecularly distinct subtype of colon cancer progresses via the recently described serrated pathway[9]. Within the pathway, the BRAF mutation is an initiating event[10]. This was shown in experiments where mice were genetically engineered to express mutated BRAF upon exposure to Villin-Cre. Whilst only 16%

of mice developed carcinomas, this increased to 56% when mutated BRAF was expressed alongside inactivated p53[10].

Table 1: FDA-approved therapies for the treatment of metastatic colon cancer

FDA-approved therapy	Mode of action
5-fluorouracil	Pyrimidine analog
Oxaliplatin	Alkylating agent
Irinotecan	Topoisomerase inhibitor
Regorafenib	Tyrosine kinase inhibitor
Bevacizumab	VEGF-A monoclonal antibody
Aflibercept	Decoy receptor for VEGF-A, VEGF-B and PIGF
Cetuximab	EGFR monoclonal antibody
Panitumumab	EGFR monoclonal antibody

Table reproduced from REF 4
Abbreviations: FDA- US Food and Drug Administration; EGFR- Epidermal growth factor receptor; VEGF- Vascular endothelial growth factor; PIGF- Placental growth factor

The BRAF mutated subtype of colon cancer is particularly aggressive and unresponsive to current treatment[11]. On current treatment regimes, patients with metastatic BRAF colon cancer have a median survival of 10 months, compared to 30-40 months for patients with wild-type BRAF[12]. Furthermore, there are currently no effective targeted treatment options for BRAF colon cancer[13]. As chemotherapy is associated with high rates of toxicity and fundamentally lacks the ability to control disease, new targeted combination strategies are needed to control this chemo-resistant subtype of colon cancer.

1.2 Physiological function of BRAF

The serine/threonine RAF kinases (A, B and C) are part of the mitogen-activated protein kinase (MAPK) cascade, which functions to control cellular proliferation, survival and differentiation in response to receptor ligand binding (Fig 2)[14]. Whilst each RAF isoform functions in MAPK signaling, the BRAF isoform is the main activator of MAPK/ERK kinase (MEK). The MAPK pathway is activated when a ligand binds to its cognate receptor, which is usually a receptor tyrosine kinase (RTK)[14]. Ligand binding results in RTK dimerisation and activation, resulting in the recruitment of Growth factor receptor-bound protein 2 (GRB2) and Son of Sevenless protein (SOS) to the cell membrane[15]. SOS functions as a RAS-specific guanine nucleotide exchange factor that catalyses the exchange of guanosine diphosphate

(GDP) for guanosine triphosphate (GTP). Active GTP-bound RAS then activates the BRAF kinase through the phosphorylation of key residues and by catalysing RAF dimerisation[16]. RAF homo and heterodimers (BRAF-BRAF or BRAF-CRAF) then phosphorylate and activate MEK1 and MEK2, which in turn phosphorylate and activate Extracellular signal-regulated kinase (ERK) 1 and ERK2[17].

The end result of the RAS-RAF-MEK-ERK signaling cascade is the phosphorylation of over 160 different cytoplasmic and nuclear proteins by ERK[18]. These include the p90 ribosomal S6 kinase, paxillin, BIM protein and various transcription factors such as c-MYC and c-JUN[16]. Thus, ERK activity induces the expression of many genes that are required for cell cycle progression, differentiation, migration, survival and proliferation. As ERK output controls many cellular processes, its activity is tightly regulated by a complex series of negative feedback loops[19]. Negative feedback is mediated by ERK, which phosphorylates many targets throughout the MAPK pathway. For example, ERK phosphorylates EGFR, CRAF, SOS1 and MEK1[20]. Phosphorylation of these proteins at specific residues results in their degradation.

1.3 BRAF mutation

In 1983, it was shown that retroviruses carrying the RAF oncogene could transform mouse cells *in vivo*[21]. However, it wasn't until 2002, during systematic genetic screening of different cancer cell lines, that BRAF mutations were discovered to occur at high frequency in melanoma cells (50-60%)[22]. Since this discovery, BRAF mutations have been identified in a variety of other cancer types such as colon cancer (10-15%), papillary thyroid cancer (40-60%), lung adenocarcinoma (3-5%), and hairy cell leukemia (100%)[23]. Whilst over 40 BRAF mutations have been discovered in human cancers, the BRAF V600E mutation occurs in approximately 95% of cases. BRAF V600E results from a transversion of thymidine to adenosine at nucleotide position 1,799 within the BRAF gene[22]. The resultant BRAFV600E protein becomes constitutively active, with its kinase activity reported as 480-fold times higher compared to wild-type BRAF[8,24].

Mechanistic insight into how the V600E mutation hyper-activates BRAF can be obtained by observing the crystallographic structures of wild-type BRAF and BRAF V600E (Fig 1)[25]. In the absence of active Ras, wild-type BRAF is folded into an inactive conformation where the nucleotide-binding pocket is buried beneath the surface of the protein, preventing access to ATP. This inactive conformation is stabilised by strong hydrophobic interactions between

residues L597 and V600 in the A-loop and residues G466, F468 and V-471 in the P-loop[26]. However, in the presence of active Ras, reversible phosphorylation occurs on residue T599 within the A-loop. The presence of the negative phosphate group disrupts the hydrophobic interactions, allowing ATP access to the nucleotide-binding pocket. Once activated, BRAF has a limited amount of time to activate MEK before phosphatases return it to its inactive conformation[27].

In contrast to wild-type BRAF, the BRAF V600E mutation results in the substitution of valine, a relatively small and hydrophobic amino acid, for glutamic acid, a large and charged amino acid[16]. This substitution disrupts the hydrophobic interactions between the A-loop and P-loop, destabilising the inactive conformation and resulting in permanent BRAF kinase activity (Fig 1; 2)[16]. Essentially, in the same way that a phosphate group disrupts the hydrophobic interactions and activates BRAF, so too does the glutamic acid substitution.

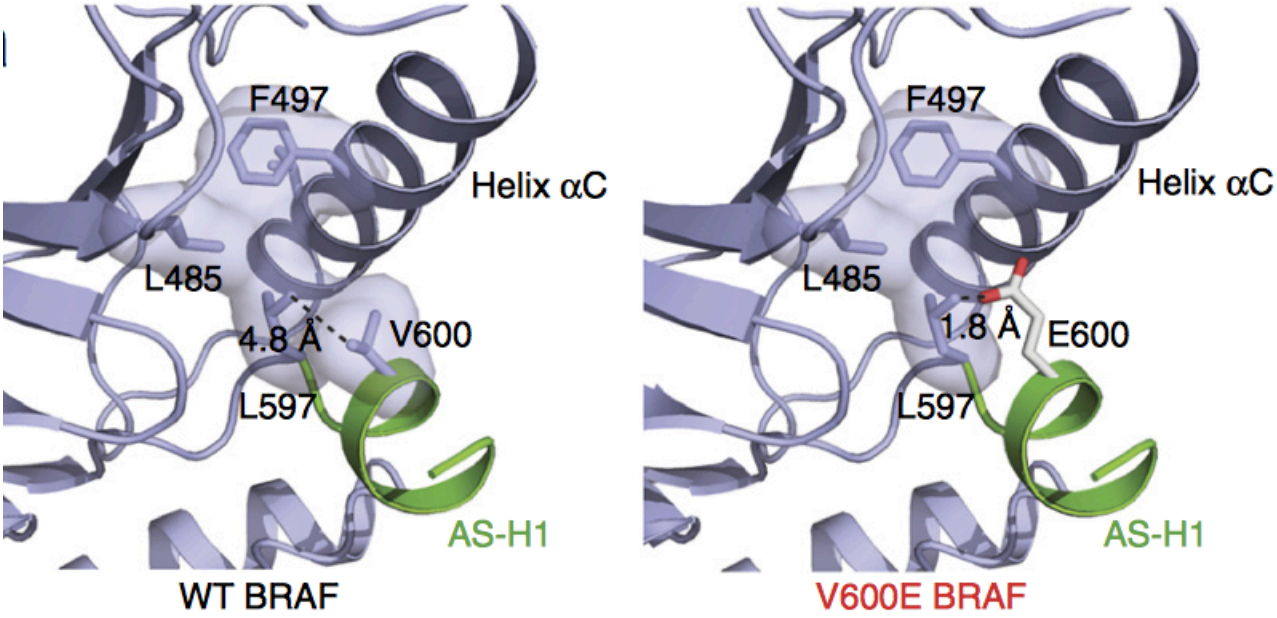

Figure 1: Crystal structures of a wild-type BRAF monomer and a BRAF V600E monomer. The effect of the V600E mutation is that it disrupts the hydrophobic interactions around the A-loop such as the interaction between V600 and L597. Figure reproduced from REF 25. Abbreviations: AS-H1- activation segment helix 1

Whilst wild-type BRAF requires dimerisation for its activity, BRAF V600E functions as a monomer[28]. This was demonstrated by the ability of recombinant BRAF V600E mutants that lack the dimerisation interface to maintain levels of ERK phosphorylation within cells[29]. The high levels of ERK output in BRAF V600E cells leads to strong ERK-mediated negative

feedback[20]. As a result, RTK's such as the EGFR are suppressed, leading to low levels of GTP-bound Ras within cells. As active Ras is responsible for catalyzing RAF dimerisation, low levels of GTP-bound Ras results in BRAF V600E functioning primarily as a monomer[28]. As BRAF V600E does not rely on Ras activity for dimerisation, it is therefore exempt from the inhibitory regulation of ERK-mediated negative feedback. Effectively, ERK signaling is dependent on BRAF V600E alone and is not affected by signaling upstream of BRAF. The fact that monomeric BRAF V600E maintains its function in the presence of low GTP-bound Ras has important implications for its treatment with BRAF inhibitors.

1.4 BRAF inhibitors

When BRAF V600E was first discovered in 2002, the only available kinase inhibitor with any activity against the mutation was sorafenib[30]. However, the concentrations of sorafenib needed to inhibit BRAF V600E was such that many off-target kinases were also inhibited, resulting in toxicity[30]. The lack of specificity resulted in ERK signaling being equally inhibited in both BRAF wild-type and BRAF V600E cells[31]. These results prompted efforts to develop more selective BRAF inhibitors.

In 2008, the first selective BRAF V600E inhibitor vemurafenib was developed[32]. Vemurafenib has an IC_{50} of 31nM against BRAF V600E, which is approximately 10 fold lower than its IC_{50} for wild-type BRAF[33]. Shortly after, the more potent and second-generation BRAF V600E inhibitor dabrafenib was developed[34]. Dabrafenib has an IC_{50} of 0.8nM against BRAF V600E, which is 4 fold lower than its IC_{50} for wild-type BRAF[34]. Much of the clinical efficacy shown by these drugs is due to their high selectivity for mutant BRAF. For example, in a phase I clinical trial on BRAF melanoma patients, phospho-ERK (pERK) levels were shown to be reduced by 80-95% in patients that had shown tumor regression after 2 weeks of treatment[35]. These results established that almost complete inhibition of pERK was necessary to cause tumor shrinkage. In contrast, less selective inhibitors such as sorafenib were unable to elicit such high levels of ERK inhibition, most likely due to their dose-limiting toxicities caused by the inhibition of off-target kinases[30].

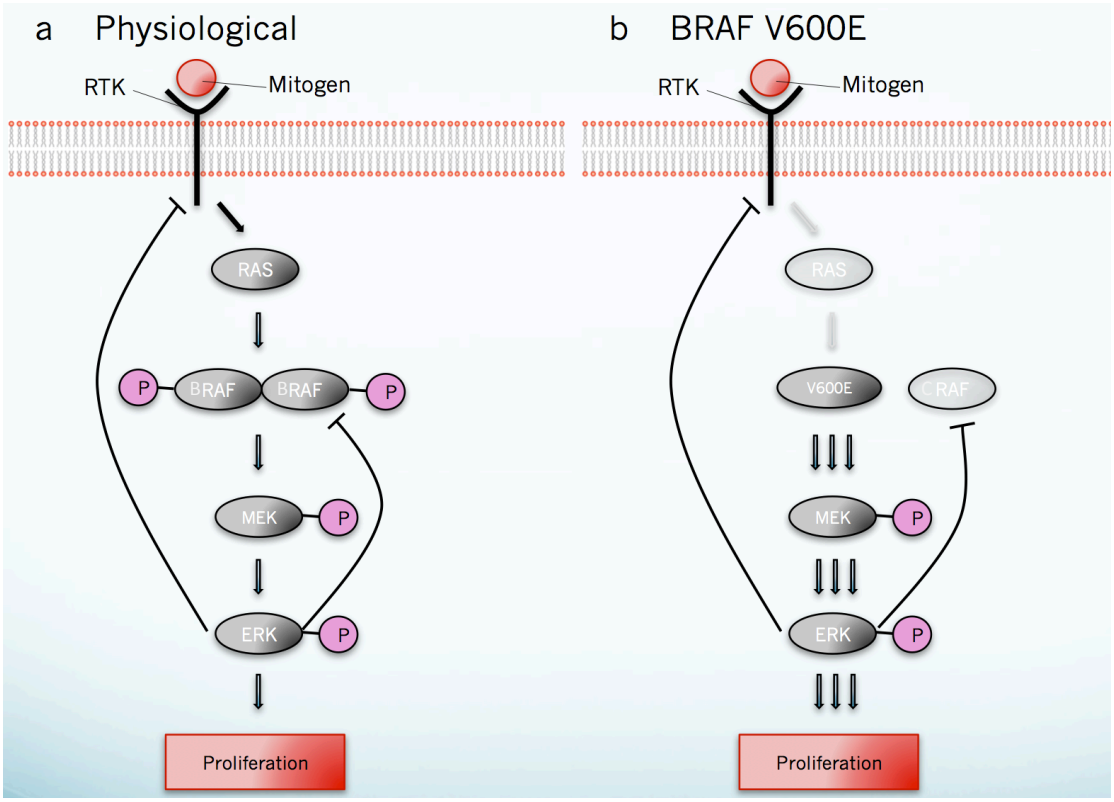

Figure 2: The MAPK cascade under physiological conditions and in BRAF V600E tumors. a) Mitogens induce conformational changes within RTK's that allows them to activate RAS. Active GTP-bound RAS can then activate RAF by catalysing its phosphorylation and dimerisation. The phosphorylated RAF dimers then activate MEK, which in turn activate ERK. ERK phosphorylates a multitude of substrates throughout the cell, which triggers cell proliferation. ERK activity also results in a negative feedback loop, where the inhibitory phosphorylation of RAF and RTK residues suppresses MAPK pathway activity. b) In BRAF V600E tumors, hyper-activated ERK induces strong negative feedback. However, BRAF V600E can continue to function as a monomer in the presence of the negative feedback, resulting in uncontrolled cell proliferation. Figure adapted from REF 16, Nature Publishing Group.

The high selectivity of dabrafenib and vemurafenib is largely due to a paradoxical phenomenon where ERK levels are inhibited in BRAF V600E cells but activated in BRAF wild-type cells[16]. In BRAF wild-type cells, the MAPK pathway is operating at physiological levels, thus there is relatively little ERK-mediated negative feedback. As such, there are still sufficient levels of active GTP-bound Ras to catalyse the formation of RAF dimers. Paradoxical activation is induced when a BRAF inhibitor binds to one partner of the RAF dimer[36]. Inhibitor binding induces a conformational change in the drug-bound partner, which allosterically activates the other non drug-bound partner. The activated dimer can then function through MEK to activate ERK. This paradoxical activation was demonstrated in experiments where kinase

impaired BRAF, representing the drug-bound BRAF partner, was transfected into BRAF wild-type cells[37]. The presence of the kinase impaired BRAF increased levels of pERK. However, at saturating concentrations of BRAF inhibitor, both RAF partners will be bound and inactivated[38].

In contrast to BRAF wild-type cells, BRAF V600E cells exhibit high levels of ERK-mediated negative feedback, which results in low concentrations of GTP-bound Ras. Under these conditions, BRAF V600E exists predominantly as a drug sensitive monomer and BRAF inhibitors are effective at inhibiting ERK signaling[16]. This model is supported by an experiment where BRAF-mutated melanoma cells were pre-treated with a MEK inhibitor before BRAF inhibitor therapy[28]. The MEK inhibitor functioned to relieve ERK-mediated negative feedback, increasing cellular concentrations of GTP-bound Ras and therefore promoting increased RAF dimerisation. As expected, the pre-treated cells were less sensitive to BRAF inhibitors. The importance of RAF dimerisation for paradoxical activation was also demonstrated in a site-directed mutagenesis study[36]. Here, the dimerisation interface of RAF kinases had been mutated to prevent dimerisation. Under these conditions, wild-type BRAF cells treated with BRAF inhibitors were resistant to paradoxical activation.

Both vemurafenib and dabrafenib have shown unparalleled clinical efficacy in BRAF melanoma patients since their introduction. In a phase III clinical trial on metastatic BRAF melanoma patients, vemurafenib showed a response rate of 48% compared to 5% for the chemotherapeutic agent decarbazine[39]. In addition, vemurafenib and dabrafenib have shown significant results in BRAF-mutated thyroid cancer, hairy cell leukemia and lung cancers[40]. Despite clinical efficacy in a range of other BRAF-mutated cancers, BRAF inhibitors have shown poor clinical efficacy in patients with BRAF colon cancer. In phase I clinical trials on BRAF colon cancer patients, only 1/19 patients showed a partial response to vemurafenib[41] and only 1/9 patients showed a partial response to dabrafenib[42].

1.5 Intrinsic resistance

In BRAF colon cancer, intrinsic resistance to RAF inhibition occurs via the formation of inhibitor-resistant RAF dimers (Fig 3)[16]. Prior to BRAF inhibition, BRAF V600E cells exhibit strong ERK-mediated negative feedback that suppresses upstream RTK's. As a result, RAS exists in its inactive GDP-bound conformation and is unable to catalyse RAF dimerisation. Consequently, BRAF V600E exists as a drug-sensitive monomer[28]. However, BRAF inhibition

blocks ERK signaling, terminating the negative feedback loop and enabling the ligand-dependent activation of RAS[43]. Active RAS stimulates the formation of RAF dimers, such as BRAF V600E-CRAF[36]. The binding of the BRAF inhibitor to one partner of the RAF dimer trans-activates the other partner, restoring MAPK pathway activity[36]. Thus, in the same way that BRAF inhibition paradoxically induces ERK activity in BRAF wild-type cells, BRAF inhibition also promotes ERK activity in BRAF V600E cells but only after ERK-mediated negative feedback has been stopped.

The rebound of ERK activity following BRAF inhibition is modest in BRAF melanoma cells but rapid in BRAF colon cancer cells[44]. Colon cancer cells exhibit rapid activation of EGFR in response to BRAF inhibition. This was demonstrated by Prahallad *et al* who performed an RNA-interference based genetic screen on BRAF colon cancer cells to determine which kinases have increased activation in response to BRAF inhibition[45]. Here, a lentiviral shRNA library, composed of the 518 human kinases was transfected into BRAF colon cancer cells. The cells were then treated with vemurafenib and the shRNA levels were recorded after a given amount of time. The shRNA corresponding to the EGFR kinase showed the highest levels of depletion. Thus, in response to BRAF inhibition, EGFR activity increases, which leads to the formation of inhibitor-resistant RAF dimers. Significantly, melanoma cells express very low levels of EGFR and forced expression of EGFR is sufficient to cause intrinsic resistance to BRAF inhibition[45].

The up-regulation of EGFR also activates the phosphoinositide 3-kinase (PI3K)/Akt pro-survival pathway[18]. Briefly, the PI3K/Akt pathway is activated when a ligand binds to its cognate receptor, which could be a RTK, such as EGFR, or a G-protein-coupled receptor (GPCR). The activated receptor then recruits the regulatory subunit of PI3K to the cell membrane, allowing the catalytic subunit to phosphorylate phosphatidylinositol 4,5-bisphosphate (PIP_2) to phosphatidylinositol 3,4,5-trisphosphate (PIP_3). PIP_3 is involved in a range of intracellular signaling networks and its activity is regulated by the phosphatase and tensin homolog (PTEN). PIP_3 binds to a variety of proteins including phosphoinositide-dependent kinase 1 (PDK1). Once bound to PIP_3, PDK1 phosphorylates Akt, which phosphorylates and activates numerous other proteins, such as mTOR, S6 kinase and GSK-3 that contribute to cell survival and proliferation. Thus, the EGFR-mediated up-regulation of this pathway contributes to the intrinsic resistance of BRAF colon cancer cells to BRAF inhibition.

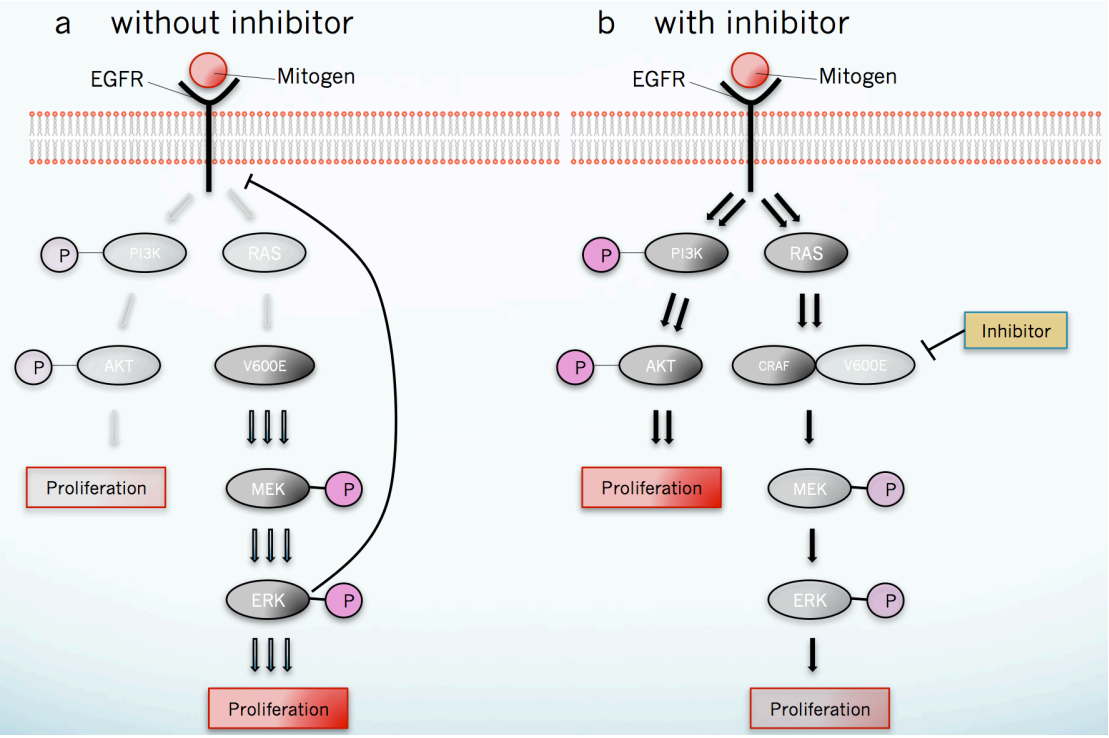

Figure 3: Effects of BRAF inhibition in BRAF V600E tumors. a) In uninhibited BRAF V600E cells, hyper-activated MAPK pathway output results in strong ERK-mediated negative feedback that suppresses upstream RAS and the parallel PI3K/Akt pathway. b) The addition of a BRAF inhibitor blocks BRAF V600E signaling, stopping ERK activity and thus terminating the negative feedback loop. Without negative feedback, activated EGFR can activate the PI3K/Akt pathway as well as RAS; both mechanisms of intrinsic resistance to BRAF inhibitors in BRAF colon cancer patients. Active RAS catalyzes the formation of inhibitor resistant RAF dimers, which sustains a low level of MAPK pathway output. Even residual amounts of ERK activity as low as 5% can be sufficient to maintain tumor growth.

1.6 Targeted combination therapies

Rational combination strategies have been developed in an effort to combat intrinsic resistance. One of the earliest combination strategies involved a BRAF/MEK inhibitor combination, designed to increase the durability of response to BRAF inhibition[46]. As inhibitor-resistant RAF dimers activate MEK, introducing a MEK inhibitor may offset the amount of time it takes for MAPK pathway reactivation. This combination strategy was also based on the success of the phase II clinical trial involving BRAF melanoma patients, who were treated with the MEK inhibitor trametinib combined with the BRAF inhibitor dabrafenib[47]. Compared to single-agent dabrafenib, patients undergoing combination treatment exhibited a higher response rate (76% vs 54%) and an increased progression-free survival (9.4 months vs 5.8 months). Significantly, after 12 months, 41% of the patients

undergoing combination treatment had not progressed compared to only 9% for single-agent treatment, highlighting the increased durability of response through this combination[47]. The BRAF/MEK inhibitor combination proved so effective that it was FDA approved for the treatment metastatic BRAF melanoma.

Whilst the BRAF/MEK clinical trial in BRAF colon cancer patients did show improved efficacy compared to single-agent dabrafenib, the results did not mirror the success of the melanoma clinical trial. In the colon cancer clinical trial, the response rate was 12%, compared to 5% for single-agent dabrafenib[46]. Of note, post-treatment analysis of patient biopsies demonstrated that pERK levels had declined compared to pre-treatment biopsies[46]. However, residual amounts of pERK expression can be sufficient to maintain tumor growth[30]. In addition, a compensatory increase in PI3K pathway output could also explain the low response rate, despite reduced pERK levels[48].

Recently, various dual or triple combination therapies involving BRAF/EGFR/MEK inhibitors have been clinically evaluated[49]. In response to BRAF inhibition, pathways downstream of EGFR become up-regulated, making them rational targets for combination therapies. Therapies that have been clinically evaluated include the combination of vemurafenib with the anti-EGFR antibody panitumumab[50], the combination of vemurafenib with the anti-EGFR antibody cetuximab[51], the combination of the BRAF inhibitor encorafenib with cetuximab[52] and the triple combination of panitumumab, trametinib and dabrafenib[53]. Of note, the vemurafenib/panitumumab combination resulted in an overall survival of 7.6 months, which is approaching the overall survival of 10 months for BRAF colon cancer patients treated with current chemotherapy regimes[50]. In addition, the panitumumab, trametinib and dabrafenib combination resulted in a preliminary response rate of 40%. Significantly, pERK was inhibited to approximately the same degree as BRAF melanoma patients treated with single-agent BRAF inhibitors.

For BRAF colon cancer patients, a response rate of 40% is highly significant. In a recent clinical trial, BRAF colon cancer patients were treated with the chemotherapy combination FOLFIRI or FOLFIRI combined with cetuximab[54]. The response rates were 13.2% and 21.9% respectively and the overall survival was 9.9 months and 14.1 months respectively, although this was not statistically significant. As BRAF colon cancer patients are currently treated with chemotherapy regimes such as FOLFIRI, the relatively high response rate achieved with the

BRAF/MEK/EGFR inhibitor combination is promising. However, the overall survival rates from the BRAF/MEK/EGFR combination are yet to be determined.

1.7 Acquired resistance

Despite initial responses, patients ultimately develop acquired resistance to BRAF inhibitor combination therapies[49]. In order to elucidate mechanisms of acquired resistance, *Ahronian et al.* developed *in vitro* models of BRAF/EGFR and BRAF/MEK inhibitor resistant VACO432 cell lines[44]. Mutations in KRAS exon 2 were identified in each of the resistant models that were not present in the sensitive cell lines. Furthermore, expressing mutant KRAS *in vitro* led to increased levels of CRAF, pMEK and pERK, indicating MAPK pathway reactivation[44]. As KRAS signaling promotes RAF dimerisation, MAPK pathway activity was likely restored through the formation of inhibitor resistant RAF dimers.

In addition to *in vitro* models, mechanisms of acquired resistance were also determined by performing whole exome sequencing on pre-treatment and post-progression patient biopsies[44]. Patients had either been treated with a BRAF/EGFR or BRAF/MEK inhibitor combination. The mechanisms of acquired resistance that were identified included KRAS amplification, BRAF amplification and a MEK1 mutation[44] (Fig 4). Both KRAS and BRAF amplifications restore MAPK pathway activity through the formation of inhibitor-resistant RAF dimers whereas the MEK1 mutation renders MEK constitutively active, by-passing its need for RAF activation[55]. However, studies on the mechanisms of acquired resistance in colon cancer patients remain limited. Further analyses of post-progression patient biopsies are needed to identify additional mechanisms of acquired resistance. Identifying these mechanisms will be helpful in developing novel strategies to overcome resistance and prolong patient survival.

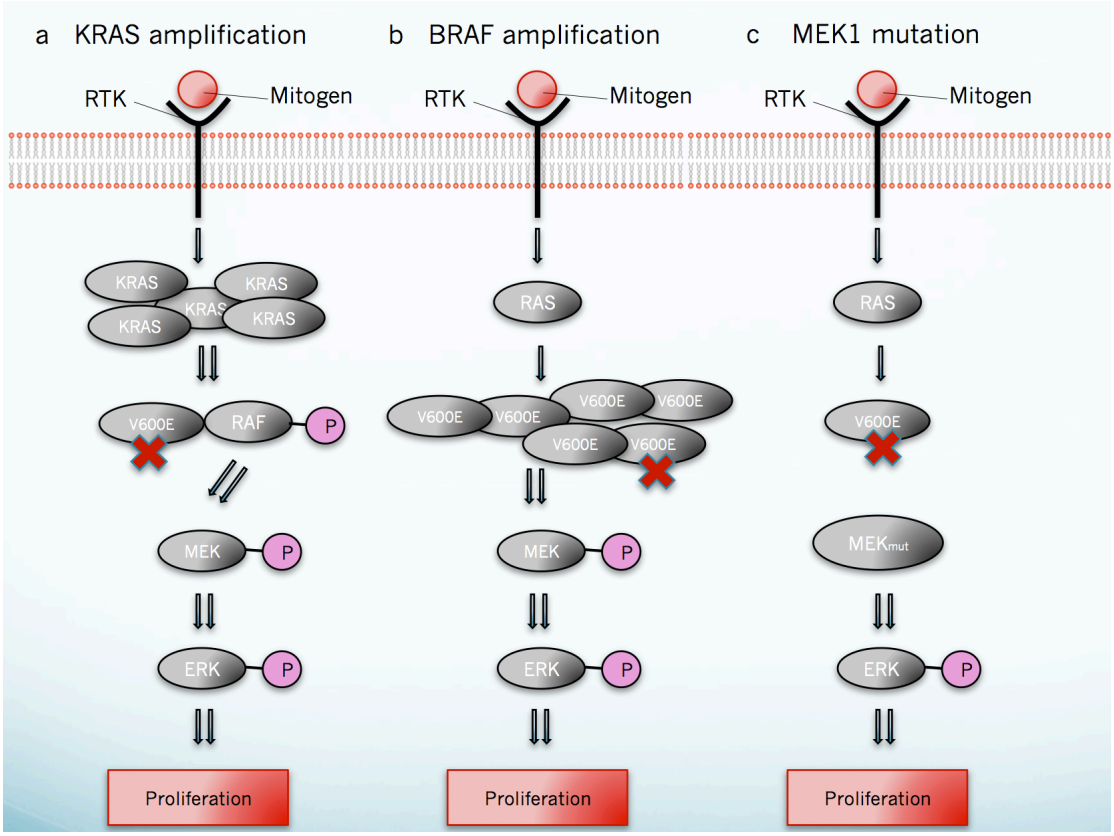

Figure 4: Mechanisms of clinically acquired resistance to BRAF/MEK and BRAF/EGFR targeted therapies in BRAF colon cancer patients. a) KRAS amplification promotes resistance via the formation of inhibitor resistant RAF dimers. b) Likewise, BRAF amplification also promotes the formation of inhibitor resistant RAF dimers. c) Activating MEK1 mutations allows MEK to activate ERK in the absence of RAF signaling.

1.8 Developing novel combination therapies: BRAF and Protein kinase CK2 inhibition

Sustainable combination therapies that can prolong patient survival relative to current treatments are desperately needed for BRAF colon cancer patients. A promising combination therapy that has not yet been tested is BRAF/protein kinase CK2 inhibition; the focus of this thesis. Protein kinase CK2 is a tetramer composed of two catalytic alpha subunits and two regulatory beta subunits[56]. Its catalytic subunits are constitutively active and are responsible for phosphorylating over 300 cellular substrates. Protein kinase CK2 is involved in the regulation of multiple signaling pathways such as the PI3K/Akt pathway, Wnt signaling and the DNA damage response. In addition, its activity has been implicated in cell cycle control, cell motility, cell survival and is associated with the maintenance of cell proliferation in tumors[57]. Protein kinase CK2 has shown elevated expression levels in a range of cancer types including leukemias, lung, breast and prostate[58].

In a recent mass spectrometry based phosphoproteomics screen, numerous protein kinase CK2 substrates were shown to be up-regulated in response to BRAF inhibition in BRAF thyroid cancer cells[57]. So in the same way that EGFR is up regulated in response to BRAF inhibition, phosphosubstrates of protein kinase CK2 are also up regulated. This up regulation could represent a distinct survival adaptation in BRAF cancer cells in response to BRAF inhibition. One of the ways that protein kinase CK2 can enhance survival is by activating AKT, which up-regulates the pro-survival output from the PI3K pathway (Fig 5)[57]. Recently, the potent protein kinase CK2 inhibitor CX-4945 entered clinical trials[58]. The combination of CX-4945 and the EGFR inhibitor erlotinib has already demonstrated efficacy in the treatment of lung cancer[59]. Furthermore, in BRAF melanoma and thyroid cancer cell lines, the combination of protein kinase CK2 and BRAF inhibition was strongly synergistic[57]. Therefore, there is strong rationale to evaluate this combination in a pre-clinical setting.

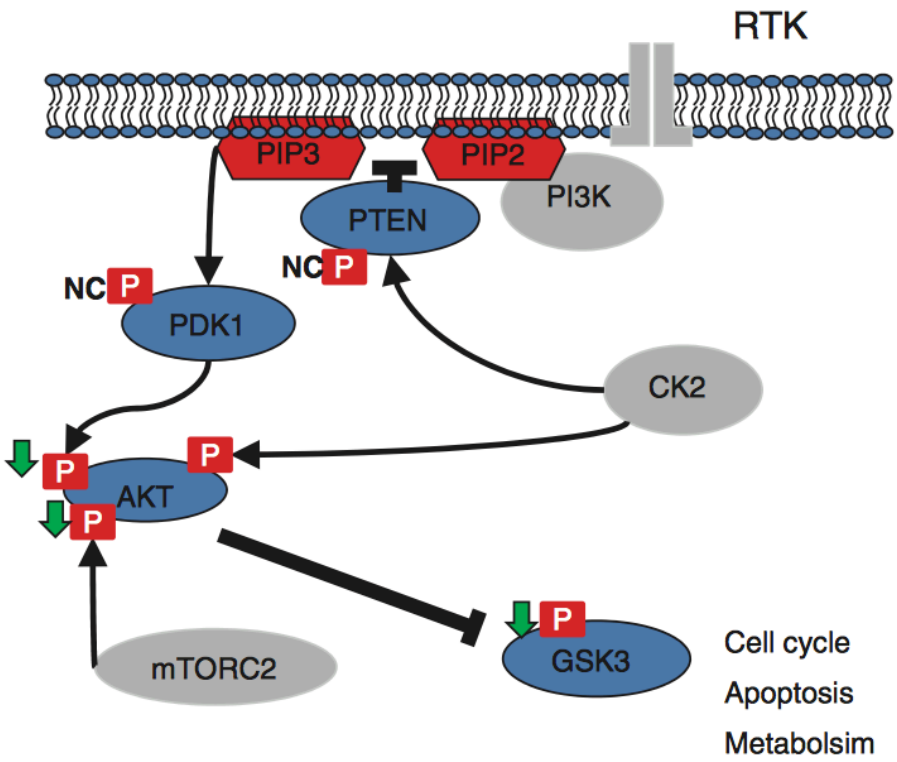

Figure 5: The influence of protein kinase CK2 on the PI3K signaling pathway. Protein kinase CK2 is constitutively active and so does not require phosphorylation for its activity. It therefore has a continuous function in activating PTEN and AKT, which increases PI3K pathway output. This activity was shown to be enhanced upon BRAF inhibition.
Figure reproduced from REF 56

1.9 Mapping cell signaling: phosphoproteomics

Many of the signaling networks within cells such as the MAPK signaling cascade are controlled by protein kinases, which add phosphate groups to serine (90%), threonine (10%) and tyrosine (0.05%) residues[60]. The reversible addition of a phosphate group to these residues results in rapid changes to protein function, allowing cells to respond quickly to external stimuli. To determine which phosphorylation events are causing a biological change in response to an external stimuli, phosphorylation events need to be quantified before and after exposure to the stimuli[60]. Many MS-based quantitation methods have been developed to quantitate these phosphorylation events[61].

However, MS-based quantitation methods are unable to detect the majority of phosphopeptides produced from a whole cell lysate sample due to their relatively low abundance compared to non-phosphorylated peptides[61]. Consequently, many phosphopeptide enrichment strategies have been developed such as immobilised metal affinity chromatography (IMAC), strong cation exchange chromatography (SCX) and metal oxide affinity chromatography (MOAC)[62]. One of the most widely used enrichment strategies and the one utilized in this study is a MOAC method that uses titanium dioxide (TiO_2) beads. This method is based on the high affinity of phosphate groups for the positively charged Ti^+ ions.

Once enriched, several MS-based methods can be used to quantitate the phosphopeptides such as stable isotope labeling of amino acids in cell culture (SILAC), isobaric tag for relative and absolute quantitation (iTRAQ) and label free quantitation. Whilst label free quantitation is inexpensive, its limitation is that each sample requires its own separate MS analysis, which increases quantitation error due to inconsistent sample preparation[60]. Phosphopeptide enrichment followed by MS-based label free quantitation was used in this study to determine how colon cancer cells respond to novel BRAF combination therapies.

1.10 Aims

The main aims of this study are to:

1. Assess the efficacy of the novel BRAF/protein kinase CK2 inhibitor combination in various BRAF colon cancer cell lines.
2. Investigate how both BRAF/protein kinase CK2 inhibition and BRAF/PI3K inhibition affects cell signaling using mass spectrometry.

1.11 Significance

There is strong rationale that BRAF/protein kinase CK2 inhibition will be effective in treating BRAF colon cancer. If this novel combination proves to be more effective in pre-clinical models compared to other targeted therapy combinations, then this provides rationale for clinical evaluation. Currently, one of the most effective targeted therapies for BRAF colon cancer is a BRAF/PI3K inhibitor combination, although this therapy is not as effective as current chemotherapy treatments. Investigating how the BRAF/PI3K and BRAF/CK2 inhibitor combinations affect cell signaling at the phosphoproteome level could offer insight into potential therapeutic targets.

2 Methods

2.1 Cell culture

Human colon cancer cell lines (Colo205, SW480, RKO and HT29) were cultured in Dulbecco's modified Eagle's medium (DMEM; Sigma Aldrich) supplemented with 10% (v/v) fetal bovine serum (FBS; Sigma Aldrich) and 1% antibiotics (10mg/mL streptomycin and 10mg/mL penicillin; Sigma Aldrich). Cells were grown in an incubator at 37°C in a humidified atmosphere of 5% CO_2. Once the cells reached 80-90% confluence, media was removed and the cells washed with phosphate buffered saline (PBS) before being detached from the flasks with trypsin (Sigma Aldrich) and seeded into new flasks. Cells were incubated with the following inhibitors; 0.015μmol/L of BRAF inhibitor (dabrafenib; Selleckchem), 4μmol/L of CK2 inhibitor (CX-4945; Selleckchem), 4μmol/L of PI3K inhibitor (GDC0941; Selleckchem) and combinations thereof for 15 minutes, 1 hour, 8 hours and 24 hours prior to harvesting for Western blot analysis and for 15 minutes prior to harvesting for phosphopeptide enrichment/mass spectrometry analysis. The inhibitor concentrations used were based on IC_{50} values determined from sensitive colon cancer cell lines (Mark Molloy's laboratory).

2.2 Cell harvesting

All colon cancer cell lines were washed three times with ice cold PBS before being harvested. Cells were harvested at 80-90% confluence by scraping cells from the base of the flask into 5mL of ice cold PBS. Cells were pelleted by centrifugation at 400xg for 4 minutes and lysed immediately or stored at -80°C for future use.

2.3 Cell lysis

Pellets were resuspended in sodium deoxycholate lysis buffer (1% (w/v) sodium deoxycholate (Sigma Aldrich), 50mM triethylammonium bicarbonate (TEAB), 1.5mM magnesium chloride (Sigma Aldrich), pH 8.0) and heated to 95°C for 2 minutes. Once the samples had cooled to room temperature, DNA was degraded by incubation with 1μL of Benzonase nuclease (Novogen, 70746) for 30 minutes. Protein concentration was determined by the micro-BCA assay (Pierce).

2.4 Western blot analysis

Protein (30μg) was mixed with 5μl of NuPAGE loading buffer (Life Technologies) and 0.4μl of dithiothreitol (10mM; Sigma Aldrich). Samples were heated at 95°C for 2 minutes and then separated by electrophoresis using a 12% Bis-Tris SDS-PAGE gel (Life technologies). Protein

was transferred onto a nitrocellulose membrane (BioRad) using the Trans-blot® Turbo™ transfer system (BioRad). Membranes were blocked for 1 hour with TBS/Tween-20 (TBS-T) containing 5% (w/v) bovine serum albumin (BSA). Membranes were incubated with primary antibodies over night at 4°C and then washed 3 times with TBS-T for 5 minutes before being incubated with fluorescently tagged (LiCor) secondary antibody for 45 minutes at room temperature. Proteins were imaged using an Odyssey system (LiCor). Primary antibodies used in this study included: mouse monoclonal anti-p44/42 MAPK (Erk 1/2; 1:2000; cat# 9107, Cell Signaling), rabbit polyclonal anti-phospho-p44/42 MAPK (Erk 1/2; Thr202/Tyr204; 1:1000; cat# 9101, Cell Signaling), rabbit monoclonal anti-Akt (Pan) (1:1000, cat# 4691, Cell signaling) and rabbit monoclonal anti-phospho S129 Akt (1:1000, cat# EPR6150, abcam). Secondary antibodies used included: IRDye 800CW Goat Anti-Rabbit IgG (1:16000; cat# 926-32211, LI-COR) and IRDye 800CW Goat Anti-Mouse IgG (1:16000; cat# 926-32210, LI-COR).

2.5 Viability assays

Cells were seeded in 96-well plates at 2000 to 5000 cells per well, with 5 replicates being used for each treatment. Cells were left for 1 hour before being placed in the incubator to avoid the edge effect. After 12 hours, media was removed and replaced with inhibitor treatments. Inhibitor treatments were; 0.015μmol/L of BRAF inhibitor (dabrafenib; Selleckchem), 4μmol/L of CK2 inhibitor (CX-4945; Selleckchem), 4μmol/L of PI3K inhibitor (GDC0941; Selleckchem), 4μmol/L of Akt inhibitor (MK-2206; Selleckchem) and dual combinations of each single agent inhibitor combined with 0.015μmol/L dabrafenib. Inhibitor concentrations were based on previously reported ID50 values[10]. Once cells in the DMSO control wells had reached 70-80% confluence, cell viability was assessed using the Presto blue assay (Life Technologies). Fluorescence was measured using the FLUOstar OPTIMA (BMG LABTECH) and cell viability calculated as the ratio of fluorescence of the treatments compared to DMSO controls. The fluorescence readings for each of the 5 replicates in each treatment were averaged and the 2 values that deviated most from the mean were excluded.

2.6 Protein digestion

Samples containing 500μg of protein were reduced using 10mM dithiothreitol (Sigma Aldrich) for 30 minutes at 60°C and then alkylated using 50mM iodoacetamide (Sigma Aldrich) for 30 minutes in the dark at room temperature. Samples were digested with trypsin (1:50μg trypsin:protein; Promega) overnight at 37°C.

2.7 Phosphopeptide enrichment

Following trypsin digestion, samples (three technical replicates for each treatment) were acidified with formic acid (2µl formic acid for every 150µl of sample) (Sigma Aldrich) and precipitated sodium deoxycholate removed via centrifugation (14500xg for 5 minutes). Samples were adjusted to 5% (v/v) trifluoroacetic acid (TFA) (Sigma Aldrich) and 76mg/ml glycolic acid (Sigma Aldrich). Three milligrams of titanium dioxide (TiO_2) beads (Titanisphere, 10µm) were washed with 5% (v/v) TFA, 80% (v/v) acetonitrile (ACN) and 76mg/ml glycolic acid. Phosphopeptides were purified by 2 consecutive incubations with washed 3mg TiO_2 beads for 30 minutes with shaking. The TiO_2 beads from the two incubations were pooled using 5% (v/v) TFA, 80% (v/v) acetonitrile (ACN) and 76mg/ml glycolic acid. TiO_2 beads were washed with 80% (v/v) ACN, 1% (v/v) TFA and then with 10% (v/v) ACN, 0.1% (v/v) TFA. Phosphopeptides were eluted from the beads with two consecutive incubations with 1% (v/v) ammonia (Sigma Aldrich) for 10 minutes with shaking. Pooled eluates were acidified with 80% (v/v) formic acid, 20% (v/v) TFA. C18 stage-tips were prepared and washed with methanol (Sigma Aldrich), then 60% (v/v) ACN, 1% (v/v) TFA and then with 0.1% (v/v) TFA. Phosphopeptides were loaded onto the stage-tips and flow-through was loaded onto a second set of stage-tips. Stage-tips were washed with 0.1% (v/v) TFA and phosphopeptides were eluted and pooled using 0.1% (v/v) TFA, 60% (v/v) ACN. Samples were dried in a SpeedVac and stored at -20°C. Prior to mass spectrometry, samples were resuspended in 0.1% (v/v) formic acid.

2.8 Mass spectrometry

Phosphopeptides were analysed using on-line C18 reverse phase nanoscale liquid chromatography (LC) tandem mass spectrometry. Samples (10µl; three technical replicates for each sample) were separated on a nanoLC system (Thermo) employing a 100-minute gradient composed of 5%–35% (v/v) ACN, 0.1% formic acid for 90 minutes, and 35-85% (v/v) ACN for 10 minutes with a flow rate of 300nl/min. The phosphopeptides were eluted and ionized into a Q-Exactive mass spectrometer (Thermo). The electrospray source was fitted with an emitter tip (10µm; New Objective, Woburn, MA) and maintained at 1.8kV electrospray voltage. Precursor ions were selected for MS/MS fragmentation using a data-dependent "Top 12" method operating in FT-FT acquisition mode with higher-energy collisional dissociation (HCD) fragmentation . FT-MS analysis on the Q-Exactive was carried out with a 70,000 resolution and an automatic gain control (AGC) target of $1x10^6$ ions in full MS. MS/MS scans were carried out at 17,500 resolution with an AGC target of $1x10^5$ ions.

Maximum injection times were set to 60 milliseconds for both full MS and MS/MS. The ion selection threshold for triggering MS/MS fragmentation was set to 10,000 counts and an isolation width of 2.0 Da was used to perform HCD fragmentation with normalised collision energy of 27%. The following parameters were enabled; monoisotopic precursor selection, charge state screening and dynamic exclusion. In addition, charge states of +1, >4, and unassigned charge states were not subjected to MS/MS fragmentation.

2.9 Database searching

Spectra files were processed using MaxQuant[63] v 1.5.3.12 using a 1% peptide and protein false discovery rate (FDR). Searches were conducted against the Swissprot_2015_6 database (selected for Homo sapiens; reviewed; 20197 entries). Searches were conducted with the following parameters; fixed modifications of carbamidomethylcysteine and variable modifications of methionine oxidation, protein amino-terminal acetylation and phosphorylation (STY). Enzyme specificity was set to trypsin and up to 2 missed cleavages was allowed. Mass tolerance for parent ions was set to +/-7 ppm and mass tolerance for fragment ions was set at +/-0.05 Da. Peptides with a charge state of +2, +3 and +4 were accepted. Spectra files were also searched against a reversed database.

2.10 Phophosite localisation and kinase assignment

MaxQuant was used to localise modifications. MaxQuant produces a probability function to determine the likelihood of a modification occurring on a specific amino acid based on the peak depth present in MS/MS spectra. Perseus[64] v 1.5.2.6 was used to putatively assign upstream kinases.

2.11 Phosphopeptide quantitation and statistical analysis

Quantitation for phosphopeptides was performed using peptide intensity from modified (STY) P-sites using Perseus v 1.5.2.6 for statistical analysis. Data was filtered to remove contaminants, reverse hits and any peptides with a phosphosite localisation probability of <0.75. Intensities were pre-processed by $\log_2$ transformation and normalised by subtracting the median. Missing values were imputed using values based on normal distribution. Data was further filtered to ensure at least two valid values in each treatment or control group. To identify differentially expressed peptides, the Student's t-test was used to compare treatments with the control. Changes were deemed significant if the q-value was <0.2 after multiple hypotheses testing using the Benjamini and Hochberg FDR method. Enriched GO

annotations and signaling pathways were identified using the Database for Annotation, visualization and Integrated Discovery (DAVID)[65,66] as well as performing Fisher exact tests within Perseus. Peptides matching enriched categories as well as having fold changes >1.5 or <1.5 were of interest.

3 Results

3.1 Response to MAPK and PI3K pathway inhibitors is mutation specific

To determine the sensitivity of the colon cancer cell lines to MAPK and PI3K inhibitors, cell proliferation was measured after inhibition with dabrafenib (BRAFi) and GDC0941 (PI3Ki). The colon cancer cell lines HT29 (BRAFV600E, PI3KP449T), Colo205 (BRAFV600E) and the BRAF/PI3K wild-type cell line SW480 were used for comparison (Fig 6A). Each cell line was treated with 0.015μmol/L dabrafenib and 4μmol/L GDC0941 for 2-5 days depending on when DMSO controls reached 80-90% confluence (Fig 6B). Both the HT29 and Colo205 cell lines that carry the BRAFV600E mutation exhibited sensitivity to BRAF inhibition (approximately 40% growth inhibition), whereas SW480 BRAF wild-type cells were not sensitive as expected (approximately 10% growth inhibition; Fig 6B). In addition, HT29 cells that have a PI3K activating mutation were sensitive to GDC0941 (approximately 60% growth inhibition) compared to the PI3K wild-type cell line SW480 (approximately 20% growth inhibition; Fig 6B). Western blots were used to confirm that cell signaling was reduced by measuring phospo-ERK1/2 and phospho-AKT (Fig 6C and D respectively). After 1 hour, phosphor-ERK1/2 output had almost disappeared in the BRAFV600E mutated cell lines, whereas no change was observed in the BRAF wild-type SW480 cell line (Fig 6C). Similarly, after 1 hour of GDC0941 exposure, Phospho-AKT Ser129 site output had almost disappeared in the PI3K mutant HT29 cell line but showed no change in the PI3K wild-type SW480 cell line (Fig 6D). Surprisingly, the PI3K wild-type Colo205 cell line showed reduction in Phospho-AKT, although this is consistent with the reduced viability of Colo205 cells to PI3K inhibition (Fig 6B).

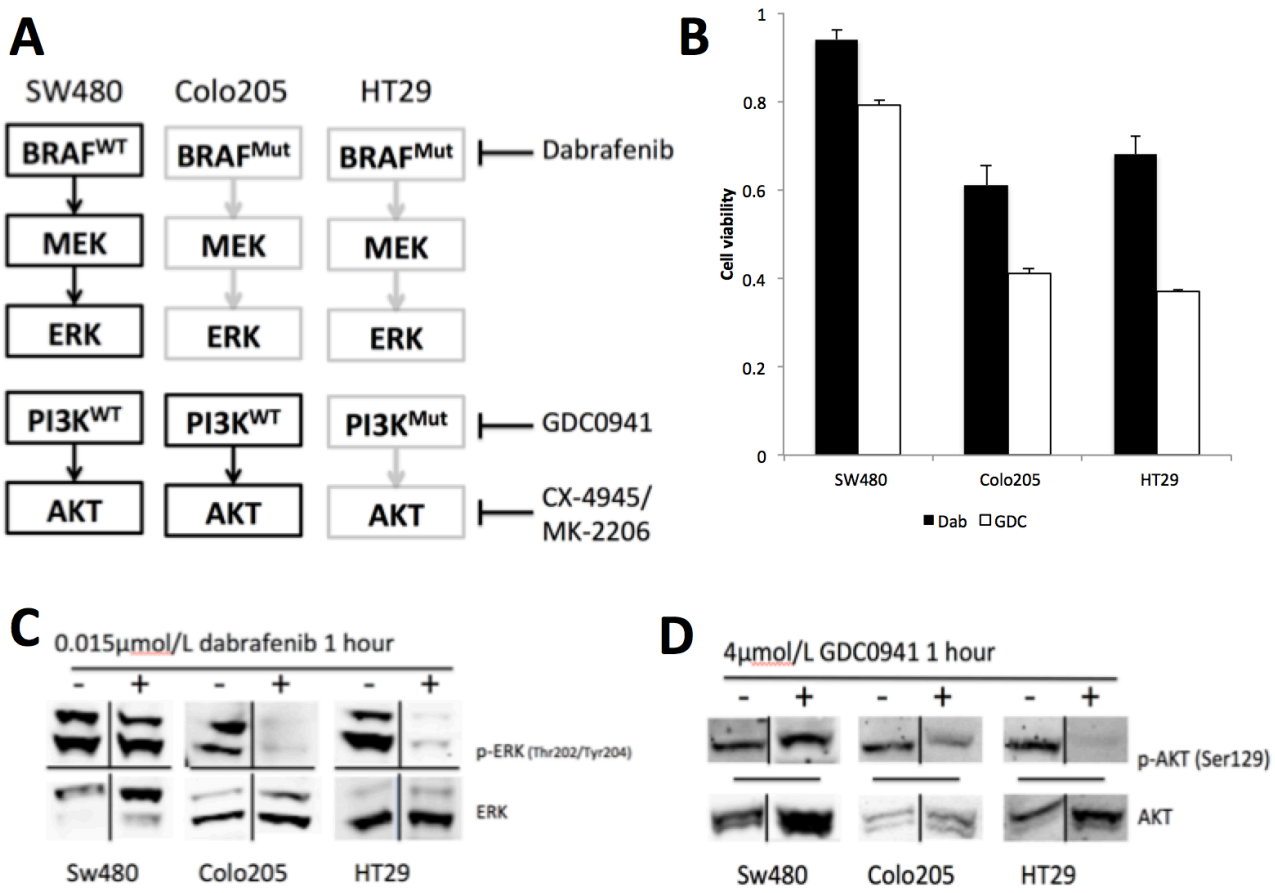

Figure 6: Colon cancer cell lines and their response to inhibitors. A, Three colon cancer cell lines were chosen based on their mutations in the MAPK pathway and the PI3K pathway. SW480 cells were chosen as they exhibit a wild-type response to both MAPK pathway and PI3K pathway inhibitors. Colo205 cells are activated by a BRAFV600E mutation but are wild type for PI3K, and HT29 cells have both a BRAFV600E mutation and PI3KP449T mutation. For each cell line, the points of inhibition by the inhibitors are shown in light grey. B, Each of the cell lines were exposed to 0.015µmol/L dabrafenib (Dab) or 4µmol/L GDC0941 (GDC) and cell viability was measured once the DMSO controls had reached 80-90% confluence; error bars, standard deviation. C, Representative western blot of Phospho-ERK Thr202/Tyr204 and total ERK output after 1 hour of exposure to 0.015µmol/L dabrafenib. D, Representative western blot of Phospho-AKT Ser129 and total AKT output after 1 hour of exposure to 4µmol/L GDC0941. Note: images from C and D were from representative gels and integrated for clarity.

3.2 Protein kinase CK2 inhibition is not effective in BRAF colon cancer cells

Previous work in the Molloy group identified a novel role for protein kinase CK2 in driving proliferation in response to BRAF inhibition in BRAF mutant melanoma and thyroid cancers, but it had not been examined in BRAF colon cancer[57]. The effectiveness of the protein kinase CK2 inhibitor CX-4945 was determined by comparing the viability of colon cancer cells after they had been exposed to a panel of inhibitors and inhibitor combinations (Fig 5A; B; C and

D). The SW480, HT29, Colo205 and RKO (BRAFV600E, PI3KH1047R) cells lines were exposed to the following inhibitors; 0.015μmol/L dabrafenib, 4μmol/L CX-4945 (CK2i), 4μmol/L GDC0941, 4μmol/L MK-2206 (AKTi) and dual combinations of each single agent inhibitor with 0.015μmol/L dabrafenib. Cell viability was determined once the DMSO control cells reached 80-90% confluence. None of the BRAFV600E mutated cell lines were sensitive to CX-4945 as a single agent, with all showing <20% growth inhibition (Fig 7B; C and D). Dual administration of CX-4945 with Dab was effective in reducing cell viability in BRAF colon cancer cells, although not as impressively as previously reported in melanoma and thyroid cancer[57]. Moreover, the combination of CX-4945 with dabrafenib was not as effective as the combination of GDC0941 with dabrafenib in any of the BRAFV600E mutated cell lines (Fig 7 B; C and D). Single agent MK-2206 was less effective than single agent GDC0941 in every cell line (Fig 7A; B; C and D). In addition, the combination of MK-2206 and Dab was significantly less effective than the combination of GDC0941 and Dab for each cell line with a PI3K mutation (Fig 7C and D). Interestingly, the combination of MK-2206 and Dab was slightly more effective than the combination of GDC0941 and Dab in the Colo205 cell line, which lacks a PI3K mutation (Fig 7B).

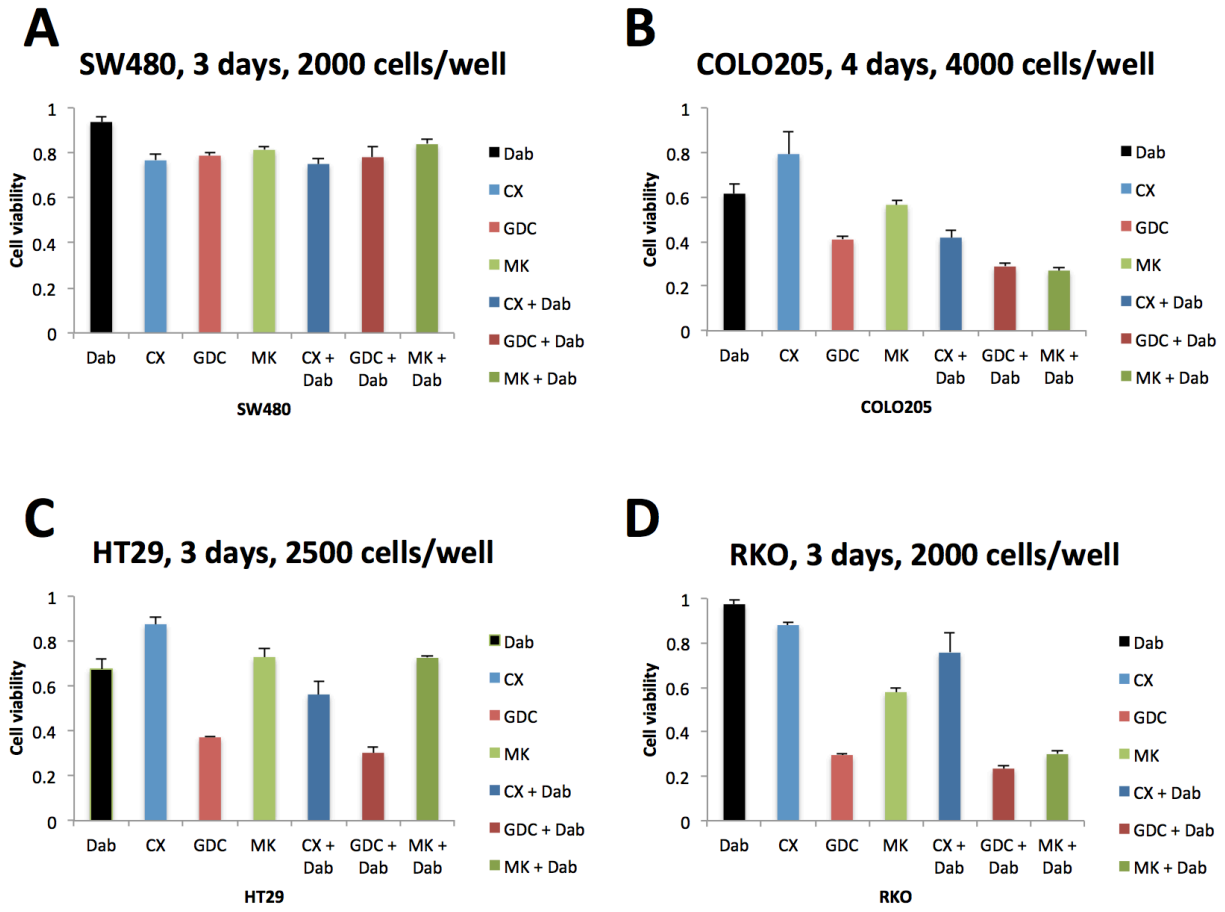

Figure 7: Cell viability assays. Cells were treated with the following inhibitors: 0.015µmol/L dabrafenib, 4µmol/L CX-4945, 4µmol/L GDC0941, 4µmol/L MK-2206 and dual combinations of each single agent inhibitor with 0.015µmol/L dabrafenib. Inhibitor treatments were applied to the cells until the DMSO control cells reached 80-90% confluence; error bars, standard deviation from 3 replicates. Cell viability assays were conducted on: A, SW480 cells. B, Colo205 cells. C, HT29 cells and D, RKO cells.

3.3 Phospho-ERK1/2 activity is rapidly reduced after exposure to MAPK and PI3K inhibitors, but rebounds after 8h

Western blot analysis of phospho-ERK1/2 output was measured after colon cancer cells were exposed to BRAF and PI3K inhibitors for 15 minute, 1 hour, 8 hour and 24 hour time points. In BRAF-mutated cell lines, phospho-ERK1/2 output declined rapidly, before being reactivated again usually by 8h (Fig 8B and C). Specifically, for each inhibitor treatment that involved dabrafenib or GDC0941 in HT29 cells, phospho-ERK1/2 output declined at the 1-hour time point and then rebounded at the 8-hour time point (Fig 8C). In contrast, no associated rebound of phospho-ERK1/2 activity was observed in the cells treated with single agent CX-4945 (Fig 8C). Similar to the HT29 cells, Colo205 cells treated with BRAF or PI3K inhibitors also showed a rebound in phospho-ERK1/2 activity, although the time points at which this

rebound occurred were not consistent across inhibitor treatments (Fig 8B). As expected, the BRAF wild-type SW480 cells showed no rebound of phospho-ERK1/2 activity upon exposure to BRAF inhibition. However, Phospho-ERK1/2 output did unexpectedly decline in these cells at the 8 and 24-hour time points (Fig 8A).

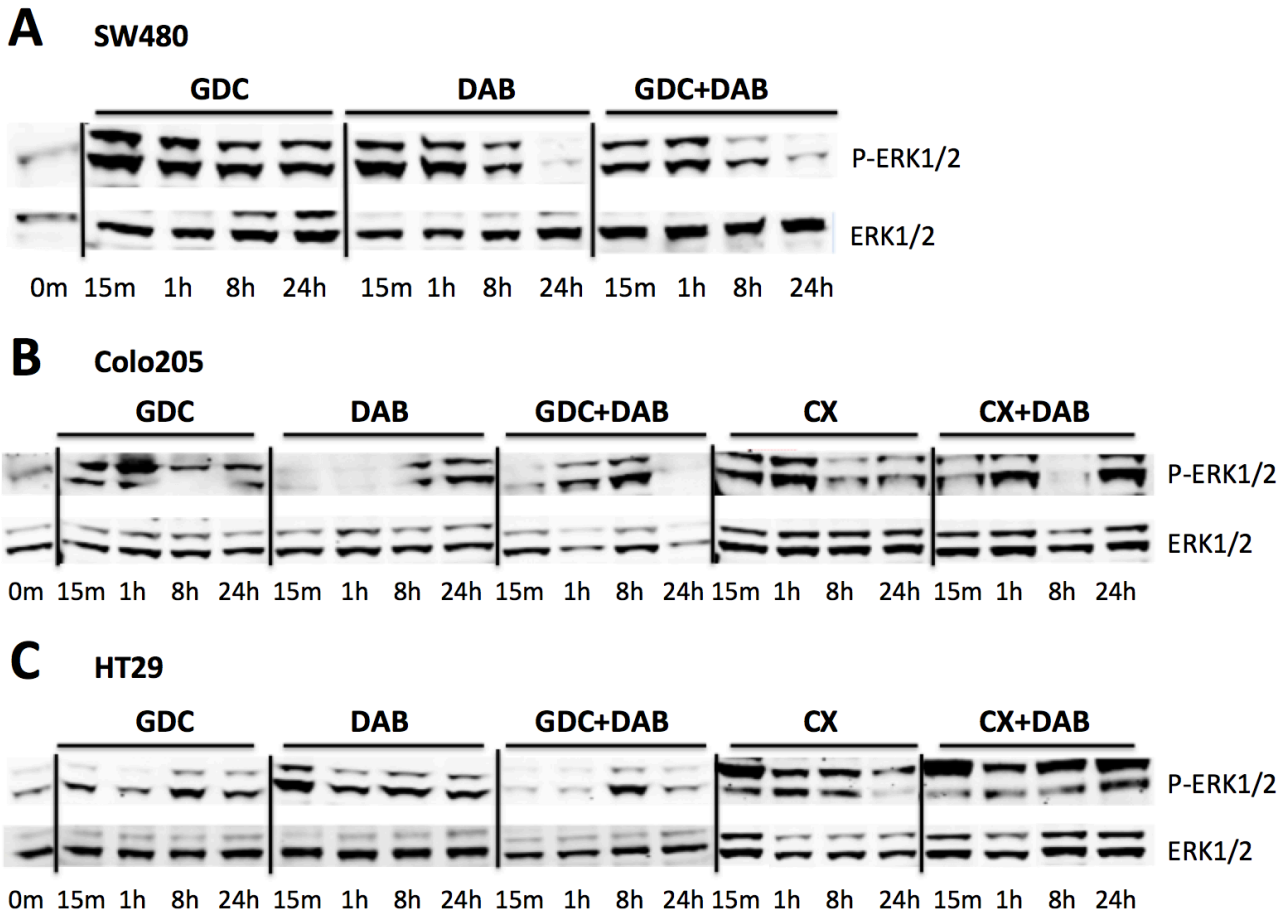

Figure 8: Western blot analysis of ERK1/2 and phospho-ERK1/2 (Thr202/Tyr204) output after exposure to inhibitors for 15 minutes, 1 hour, 8 hours or 24 hours. Western blots were performed on A, SW480 cells (n=1). B, Colo205 cells (n=1) and C, HT29 cells (n=1). Inhibitors used included 4µmol/L GDC0941, 0.015µmol/L dabrafenib, 4µmol/L CX-4945 and combinations thereof.

3.4 PI3K inhibition reduces phospho-AKT levels in PI3K-mutated cell lines

Western blot analysis of phospho-AKT (Ser129) levels was measured after colon cancer cells were exposed to BRAF and PI3K inhibitors for 15 minute, 1 hour, 8 hour and 24 hour time points. As expected, in response to PI3K inhibition, PI3K-mutated HT29 cells showed a reduction in phospho-AKT levels over the 24-hour time period, whereas in response to BRAF inhibition alone, phospho-AKT levels remained consistent (Fig 9C). When PI3K and BRAF inhibition was combined, phospho-AKT levels declined at the 8-hour time point (Fig 9C). In

contrast, single agent PI3K inhibition resulted in reduced phospho-AKT levels at the 1-hour time point. For PI3K wild-type SW480 cells, phospho-AKT levels remained relatively consistent over the 24-hour time period in response to both PI3K and BRAF inhibition (Fig 9A). In contrast, for PI3K wild-type Colo205 cells, phospho-AKT levels declined over the 24-hour period in response to PI3K inhibition (Fig 9B).

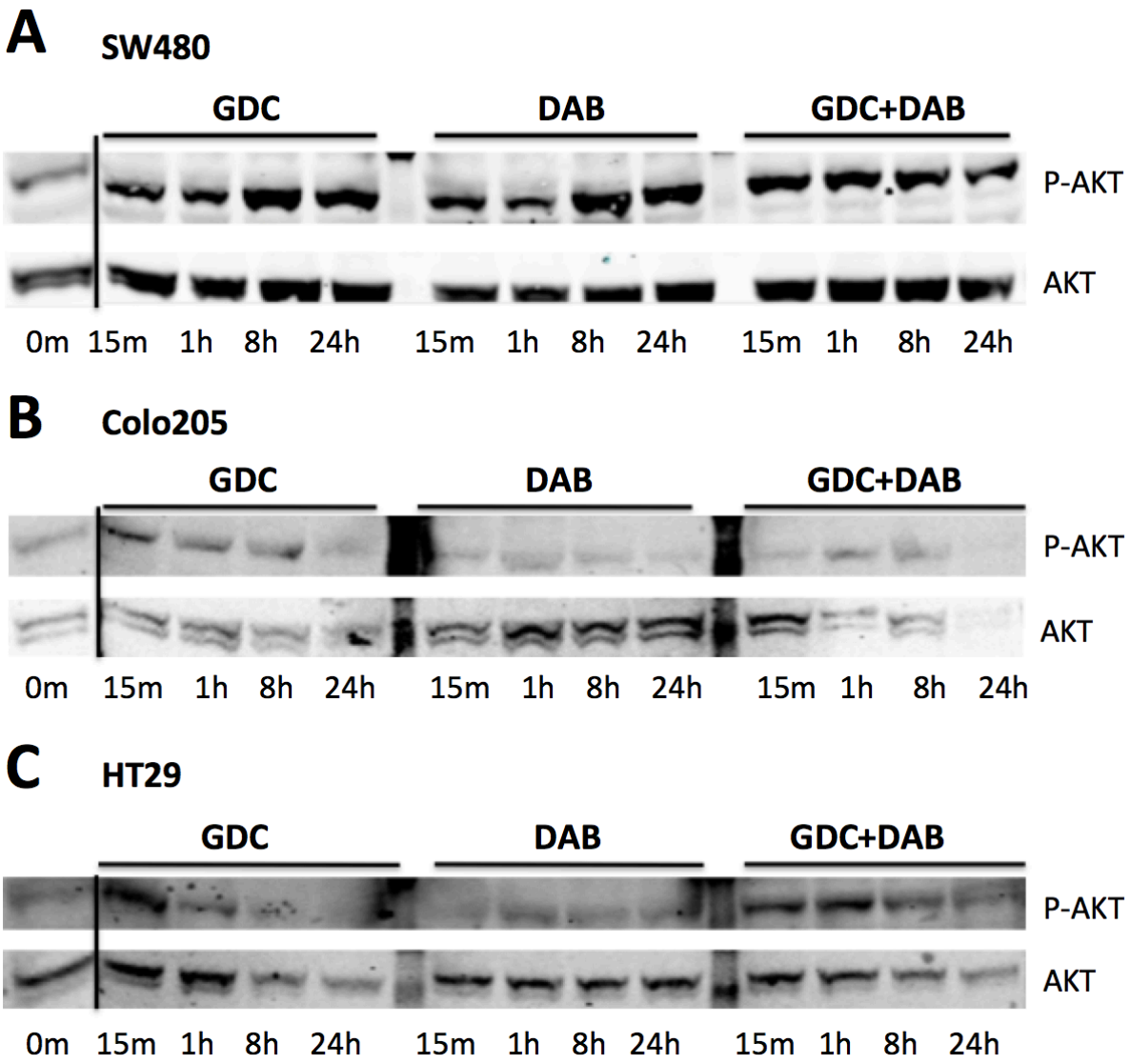

Figure 9: Western blot analysis of AKT and phospho-AKT (Ser129) output after exposure to inhibitors for 15 minutes, 1 hour, 8 hours or 24 hours. Western blots were performed on A, SW480 cells (n=1). B, Colo205 cells (n=1) and C, HT29 cells (n=1). Inhibitors used included 4μmol/L GDC0941, 0.015μmol/L dabrafenib and their combination.

3.5 Phosphoproteomic characterization of BRAF, PI3K and protein kinase CK2 inhibition

A label-free quantitative mass spectrometry study was used to examine cell signaling by studying changes in phosphopeptides following short-term drug exposure to BRAF, PI3K and

protein kinase CK2 inhibitors. Based on the Western blot data and given that a cells phosphoproteome can change rapidly, cells were harvested at 15 minutes post-drug exposure and subjected to the phosphoproteomic workflow shown in Figure 10. Briefly, proteins were extracted, digested with trypsin, phosphopeptides were enriched using TiO_2 and analysed by nanoLC-MS/MS using a Q Exactive Orbitrap mass spectrometer.

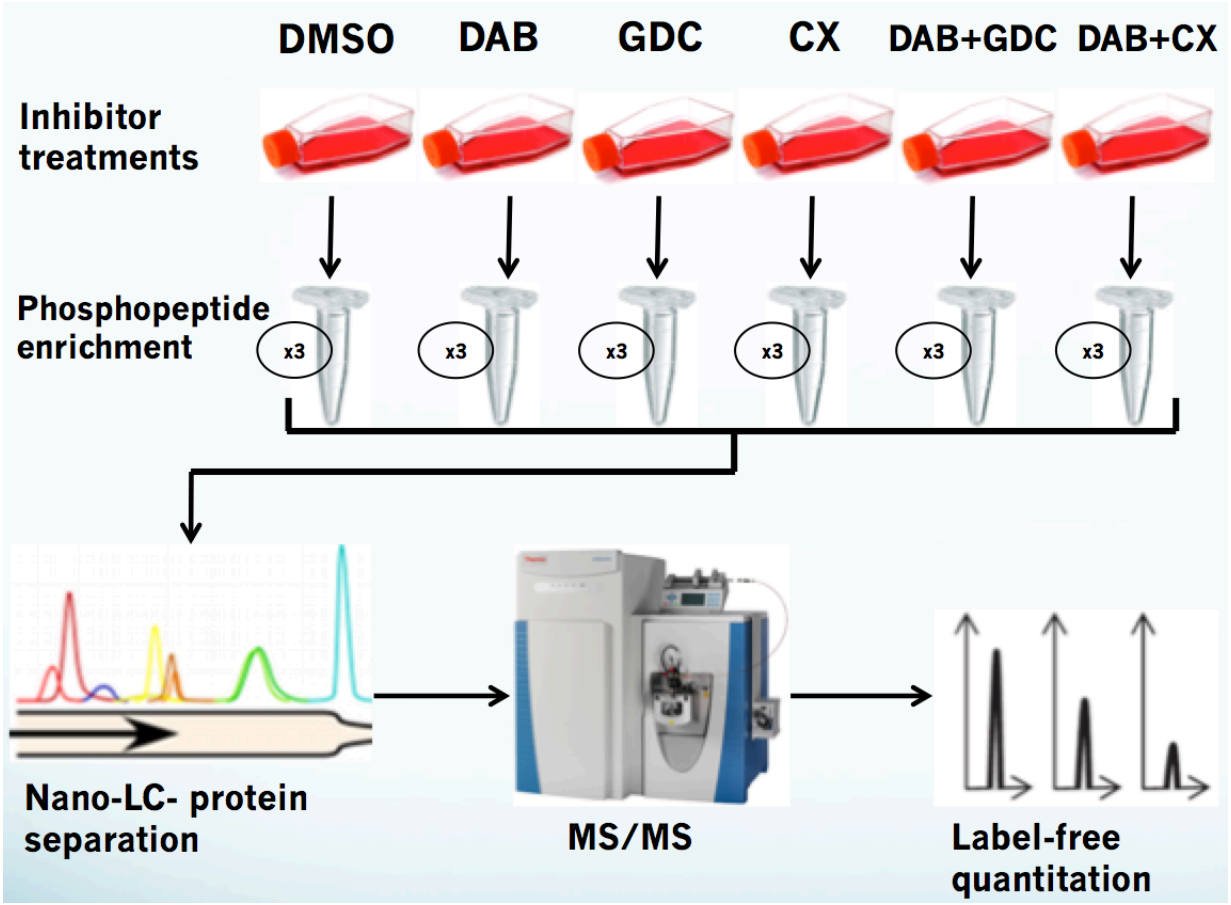

Figure 10: Phosphoproteomic workflow used to identify phosphopeptides that are differentially expressed after 15 minutes of exposure to BRAF, PI3K or CK2 inhibitors and inhibitor combinations. HT29 and Colo205 cells were exposed to the following inhibitors; 0.015µmol/L dabrafenib, 4µmol/L CX-4945, 4µmol/L GDC0941 and dual combinations of each single agent inhibitor with 0.015µmol/L dabrafenib. Cells were harvested after 15 minutes of exposure to the inhibitors and cell lysates digested with trypsin. Phosphopeptides were enriched by TiO_2 (three technical replicates for each sample) and separated by 60min nano-LC before being analysed by a Q Exactive Orbitrap mass spectrometer (MS/MS). Spectra files were entered into MaxQuant to identify and quantitate phosphopeptides by MS1 quantitation and Perseus was used to identify differentially expressed phosphopeptides between treatment groups.

In total, 4016 unique phosphopeptides were identified from the HT29 cell samples and 2148 phosphopeptides were identified from the Colo205 cell samples, both at a FDR of 1%. Within both cell samples, the number of phosphopeptides that were identified was consistent, both within treatments and across the different treatments (Table 2 and 3 respectively). In addition, within each treatment, approximately 60% of the phosphopeptides that were identified were common to all three replicates (Table 2 and 3). However, within the Colo205 cell data, relatively fewer phosphopeptides were common to all three replicates and higher coefficient of variation for some treatment groups was noted (Table 3). The differences between groups was attributed to reduced MS instrument performance as the samples were analysed at different time points.

Table 2: Number of phosphopeptides identified in HT29 cell samples

Sample	Number of phosphopeptides	SD[a]	Number of phosphopeptides common to all 3 replicates	Average CV[b] (%) for phosphopeptides with 3 valid values
Control 1 Control 2 Control 3	1987 2282 2205			
Average	2158	+/- 153	1351	35.8
Dabrafenib 1 Dabrafenib 2 Dabrafenib 3	2129 2067 1783			
Average	1993	+/- 184.5	1135	31
GDC0941 1 GDC0941 2 GDC0941 3	2259 2255 2242			
Average	2252	+/- 8.9	1511	20.2
CX-4945 1 CX-4945 2 CX-4945 3	2047 2184 2139			
Average	2123	+/- 69.8	1360	22.2
Dab + GDC 1 Dab + GDC 2 Dab + GDC 3	1965 1907 1993			
Average	1955	+/- 43.9	1111	38.2
Dab + CX 1 Dab + CX 2 Dab + CX 3	1789 2062 2140			
Average	1997	+/- 184.3	1160	21.5

a) Standard deviation. b) Coefficient of variation

Table 3: Number of phosphopeptides identified in Colo205 cell samples

Sample	Number of phosphopeptides	SD[a]	Number of phosphopeptides common to all 3 replicates	Average CV[b] (%) for phosphopeptides with 3 valid values
Control 1 Control 2 Control 3	996 1144 1077			
Average	1072	+/- 74.1	677	29.6
Dabrafenib 1 Dabrafenib 2 Dabrafenib 3	1051 1192 1085			
Average	1109	+/- 73.6	678	27.3
GDC0941 1 GDC0941 2 GDC0941 3	981 1137 1066			
Average	1061	+/- 78.1	658	32.1
CX-4945 1 CX-4945 2 CX-4945 3	980 887 1019			
Average	962	+/- 67.8	549	28.8
Dab + GDC 1 Dab + GDC 2 Dab + GDC 3	792 798 734			
Average	775	+/- 35.3	333	57.6
Dab + CX 1 Dab + CX 2 Dab + CX 3	910 789 766			
Average	822	+/- 77.4	377	41.6

a) Standard deviation. b) Coefficient of variation

To determine differences in the relative abundance of phosphopeptides treated with BRAF, PI3K and protein kinase CK2 inhibitors, phosphopeptides were quantified using MaxQuant LFQ and analysed using Perseus. Two sets of analyses' were performed. The first involved pairing each treatment group with the control and performing a Student's t-test with a permutation-based FDR of 0.2 and a fold change cutoff of +/- 1.5 (Fig 11). The second analyses' involved using a robust ANOVA with a Benjamini-Hochberg FDR of 0.05 in order to identify phosphopeptides that changed in abundance across treatment groups (Fig 12).

Table 4 shows results using the Student's t-test's on the HT29 cell data, 44 phosphopeptides were differentially expressed between the control and the dabrafenib treated cells (table 4), 34 phosphopeptides for the GDC0941 treated cells, 64 phosphopeptides for the protein kinase CK2 treated cells, 50 phosphopeptides for the dabrafenib/GDC0941 treated cells and 55 phosphopeptides for the dabrafenib/protein kinase CK2 treated cells. Within Perseus, many

of the differentially expressed phosphopeptides were annotated with roles in cytoskeletal reorganization, transcriptional control and chromatin structure. Despite these similar annotation categories, there was very limited overlap between the phosphopeptides identified across the different Student's t-test's indicative of different effects of these inhibitors on signal transduction.

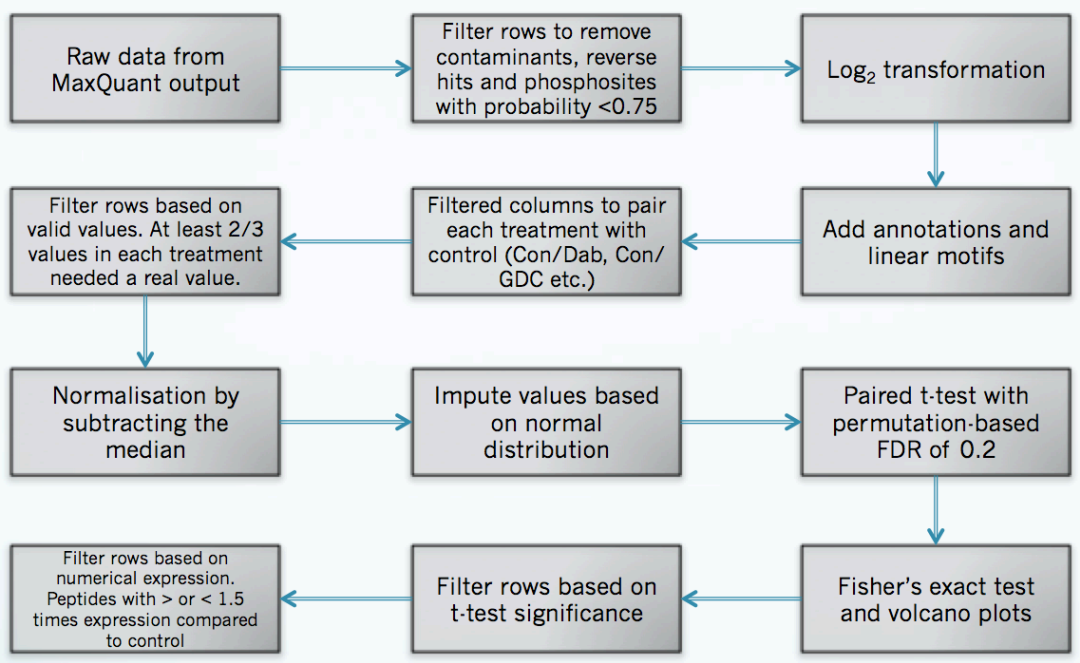

Figure 11: Perseus workflow used to perform Student's t-test's. Once the data had been filtered, transformed and normalized, each of the treatments were individually paired with the DMSO control to form five separate data groups (control/dabrafenib, control/GDC0941, control/CX-4945, control/Dab+GDC and control/Dab+CX). Student t-test's were performed on each of these groups with a permutation-based FDR of 0.2. Data was filtered to create separate matrices for both the t-test significant up-regulated and down-regulated phosphopeptides. Fisher exact tests were done to determine which motifs or annotations were significantly enriched from the t-test significant phosphopeptides (up-regulated and down-regulated separately) compared to the background list of all the phosphopeptides. Finally, the list of t-test significant phosphopeptides was filtered to contain only those that were up-regulated or down-regulated 1.5 times compared to the control.

Table 4: Differentially expressed phosphopeptides in HT29 cells after 15 minutes of BRAF inhibition

UniProt	Protein name	Amino acid	Position within protein	Localization probability	Fold change	q-value
P02545	Lamin-A/C;Prelamin-A/C	S	22	0.83	1.5	0.04
P04792	Heat shock protein beta-1	S	82	1	1.59	0
P18615	Negative elongation factor E	S	115	1	2.07	0.03
P43243	Matrin-3	S	188	1	2.31	0.04
P49006	MARCKS-related protein	S	104	1	1.75	0.03
P50402	Emerin	S	49	0.89	2.73	0.1
P58107	Epiplakin	S	2716	1	2.86	0.18
Q09666	Neuroblast differentiation-associated protein AHNAK	S	135	1	1.83	0.04
Q14160	Protein scribble homolog	S	1448	1	2.37	0.11
Q8WWI1	LIM domain only protein 7	S	1510	1	1.81	0.06
Q92597	Protein NDRG1	S	330	0.99	1.53	0.11
Q9BQ52	Zinc phosphodiesterase ELAC protein 2	S	199	1	2.14	0.13
Q9BTC0	Death-inducer obliterator 1	S	1456	1	1.54	0.03
Q9C0C2	182 kDa tankyrase-1-binding protein	S	836	1	2.04	0.11
Q9H788	SH2 domain-containing protein 4A	S	315	1	2.31	0.11
Q9UKV3	Apoptotic chromatin condensation inducer in the nucleus	S	710	1	1.54	0.09
Q9UKX7	Nuclear pore complex protein Nup50	S	221	1	2.35	0.03
Q9ULW0	Targeting protein for Xklp2	S	738	1	1.9	0.04
Q9Y446	Plakophilin-3	S	314	1	1.52	0.02
P42167	Lamina-associated polypeptide 2, isoforms beta/gamma	T	208	1	2	0.05
P55265	Double-stranded RNA-specific adenosine deaminase	T	601	0.99	2.04	0.06
Q6ZMW2	Zinc finger protein 782	T	583	0.95	3.05	0.2
P06400	Retinoblastoma-associated protein	S	807	1	1.86	0.05
P06400	Retinoblastoma-associated protein	S	811	1	2.14	0.07
Q6PJG2	ELM2 and SANT domain-containing protein 1	S	661	1	1.87	0.11
Q9BVC5	Ashwin	S	189	1	2.18	0.2
P13639	Elongation factor 2	T	57	1	2.82	0.06
P13639	Elongation factor 2	T	59	1	2.49	0.04
Q6PJG2	ELM2 and SANT domain-containing protein 1	T	655	0.99	1.96	0.08
Q7Z417	Nuclear fragile X mental retardation-interacting protein 2	T	571	0.50	-1.71	0.13
P18583	Protein SON	S	2013	1.00	-1.70	0.19
P55196	Afadin	S	1182	1.00	-1.53	0.19
Q01518	Adenylyl cyclase-associated protein 1	S	308	0.93	-2.12	0.17
Q15424	Scaffold attachment factor B1	S	601	1.00	-1.56	0.00
Q15424	Scaffold attachment factor B1	S	604	1.00	-1.56	0.00
Q5T1M5	FK506-binding protein 15	S	1164	1.00	-1.59	0.20
Q8NC56	LEM domain-containing protein 2	S	138	0.96	-1.92	0.11
Q8NC56	LEM domain-containing protein 2	S	139	0.98	-2.30	0.18
Q8TF01	Arginine/serine-rich protein PNISR	S	670	1.00	-1.59	0.19
Q9ULL5	Proline-rich protein 12	S	560	0.98	-1.74	0.19
Q9ULL5	Proline-rich protein 12	S	561	0.98	-1.80	0.20
Q9UQ35	Serine/arginine repetitive matrix protein 2	S	2067	1.00	-1.72	0.04
Q9UQ35	Serine/arginine repetitive matrix protein 2	S	2071	1.00	-2.06	0.11
Q9UQ35	Serine/arginine repetitive matrix protein 2	S	1890	1.00	-1.59	0.11

The Perseus workflow for performing the ANOVA analysis is shown in figure 12. For the HT29 data, the ANOVA of the control, dabrafenib, GDC0941 and Dab+GDC treatment groups identified 48 differentially expressed phosphopeptides (Supplementary table 12). The ANOVA of the control, dabrafenib, protein kinase CK2 and Dab+CK2 treatment groups identified 59 phosphopeptides (Supplementary table 13). For the Colo205 data, the ANOVA of the control, dabrafenib, GDC0941 and Dab+GDC treatment groups identified 23 phosphopeptides (Supplementary table 14) and the ANOVA of the control, dabrafenib, protein kinase CK2 and Dab+CK2 treatment groups did not identify any phosphopeptides.

The intensities of ANOVA-significant phosphopeptides from each of these analyses' were normalized by z-scoring and then visualized by hierarchical clustering (Fig 13 and 14). The majority of the phosphopeptides were either all up-regulated or all down-regulated in each treatment group compared to the control. The phosphopeptides that were deemed of interest were the few that were up-regulated in some treatment groups but down-regulated in others. For example, phosphosite T646 from the multidrug resistance-associated protein 4 (UniProt: O15439) was up-regulated in the dabrafenib treatment group but down-regulated in the GDC0941 and Dab+GDC treatment groups (Fig 13). Likewise, phosphosite S2559 from the chromodomain-helicase DNA binding protein 7 (UniProt: Q9P2D1) was up-regulated in the dabrafenib treatment group but down-regulated in the GDC0941 and Dab+GDC treatment groups (Fig 13). PhosphoSitePlus[67] was used to help find the biological significance of these interesting phosphorylation sites. However, there is a paucity of information regarding the biological function of these phosphosites.

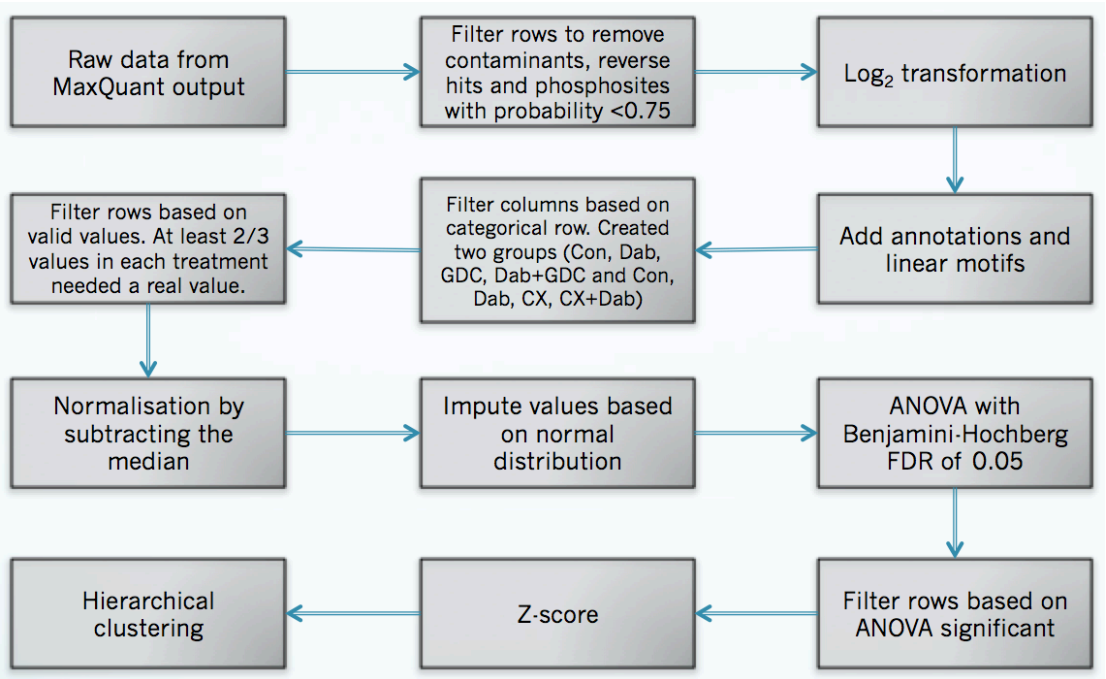

Figure 12: Perseus workflow used for ANOVA analysis. Once the data had been filtered, transformed and normalized, two separate groups were created. One group consisted of control, dabrafenib, GDC0941 and Dab+GDC and the other group consisted of control, dabrafenib, CX-4945 and Dab+CX. ANOVA analysis was performed on each of these groups with a Benjamini-Hochberg corrected FDR of 0.05. Data was then filtered to contain only the ANOVA significant phosphopeptides and Z-scored before hierarchical clustering.

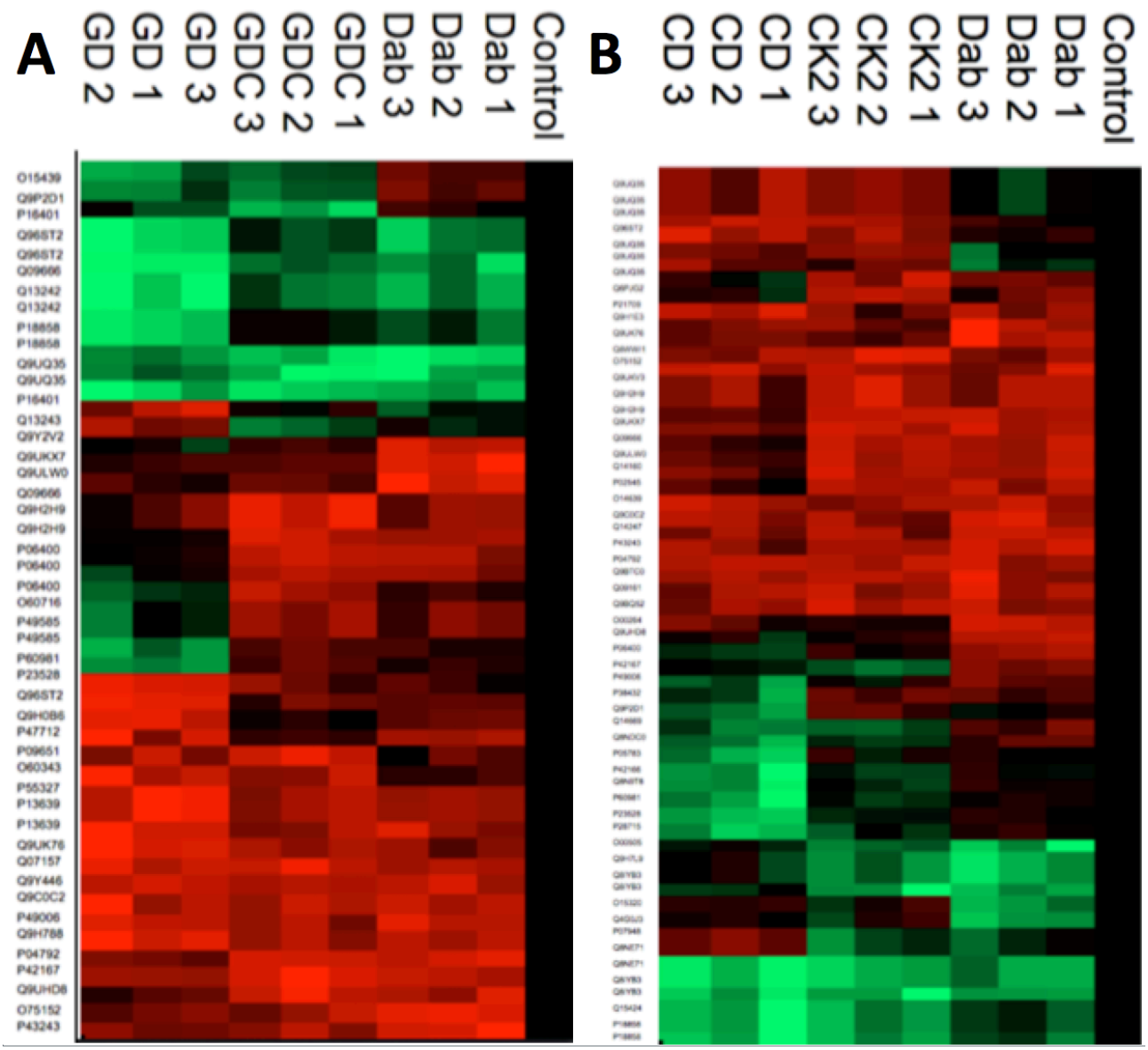

Figure 13: Hierarchical clustering on the ANOVA-significant phosphopeptides from the HT29 cell samples. Following ANOVA analysis with a Benjamini-Hochberg corrected FDR of 0.05, the average was taken of the 3 control replicates and this value was set at 0, with the other treatments being normalized according to this value. A, hierarchical clustering on the control, dabrafenib, GDC0941 and Dab+GDC cells samples. B, hierarchical clustering on the control, dabrafenib, CX-4945 and Dab+CX cells samples. (red > 0, green < 0).

Abbreviations: Dab- Dabrafenib; GDC- GDC0941; GD- GDC0941 and Dabrafenib; CK2- CX-4945; CD- CX-4945 and Dabrafenib

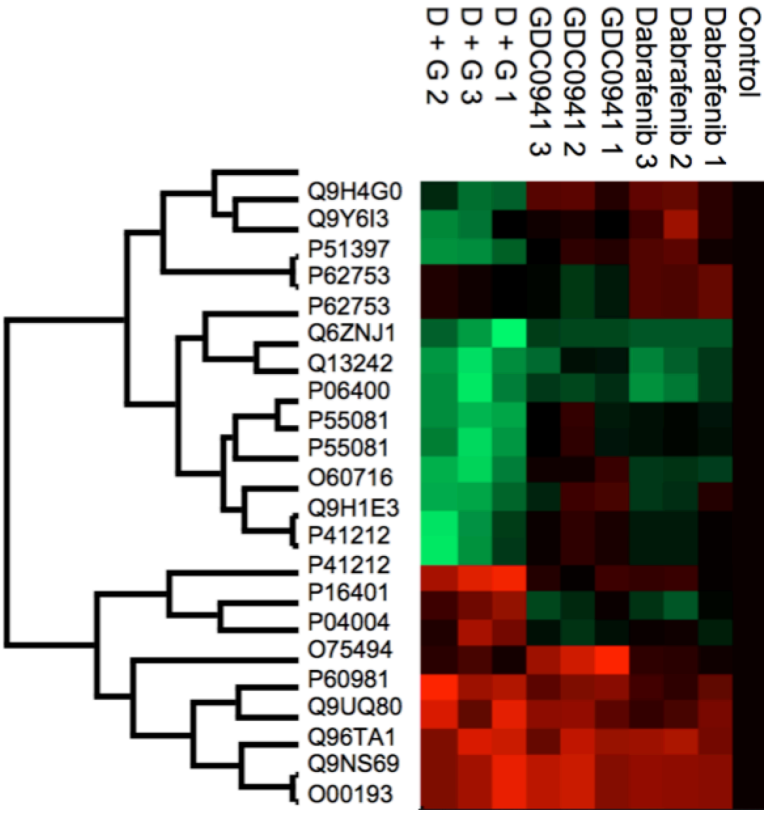

Figure 14: Hierarchical clustering on the ANOVA-significant phosphopeptides from the Colo205 cell samples. Following ANOVA analysis with a Benjamini-Hochberg corrected FDR of 0.05, the average was taken of the 3 control replicates and this value was set at 0, with the other treatments being normalized according to this value. Hierarchical clustering was performed on the control, dabrafenib, GDC0941 and Dab+GDC (D+G) cells samples. (red > 0, green < 0).

Abbreviations: G + D- GDC0941 + Dabrafenib

3.6 Kinase enrichment analysis

Within Perseus, motif analysis was performed on the phosphopeptides with the highest confidence phosphosite assignments (>0.75) in order to identify kinases most likely to be responsible for substrate phosphorylation. Based on the Student's t-test data, Fisher exact tests were used to determine which kinases were enriched at least 1.5-fold in either the up-regulated or down-regulated phosphopeptide lists compared to the background of the entire dataset. The Fisher exact tests were done with a permutation-based FDR of 0.2 for each of the treatment groups within the HT29 cell data, including dabrafenib (Table 5 and Supplementary table 1), GDC0941 (Table 6 and Supplementary table 2), protein kinase CK2 (Supplementary table 3), Dab+GDC (Table 7 and Supplementary table 4) and Dab+CK2 (Supplementary table 5 and Supplementary table 6). Fisher exact tests were also performed on Colo205 cell data but

the only treatment group that gave significant results was the up-regulated phosphopeptides from the dabrafenib treatment (Supplementary table 7).

For the HT29 data, MAPK pathway kinases were enriched in the list of phosphopeptides that had been down-regulated in response to BRAF inhibition or combined BRAF/PI3K inhibition (Supplementary table 1 and Supplementary table 4). Kinases such as ERK1 and ERK2 were enriched 1.98-fold and the RAF1 (CRAF) kinase was enriched 4.11-fold in these phosphopeptide lists. In addition, for the phosphopeptides that had been up-regulated in response to PI3K inhibition, many of the enriched kinases were related to the MAPK pathway (Table 6). Kinases such as the Src kinase was enriched 7.67-fold and the RAF1 kinase was enriched 3.07-fold in this phosphopeptide list, probably as a compensatory response to PI3K inhibition. For the list of phosphopeptides that were up-regulated in response to BRAF inhibition, there was no enrichment of protein kinase CK2 substrate motifs, as was the case with previous findings using BRAF thyroid cancer cells[57] (Table 5). Rather, 58% of the kinases that were enriched from this phosphopeptide list were regulated by the EGFR (Fig 15). In contrast, only 24% of the kinases from the list of phosphopeptides that were down-regulated in response to BRAF inhibition were EGFR-regulated (Fig 15). This data points to the obvious need to control EGFR signaling in BRAF colon cancer.

Table 5: Over-represented annotation categories from the phosphopeptides that were up-regulated in response to BRAF inhibition in HT29 cells

Category column	Category value	Total size	Selection size	Category size	Intersection size	Enrichment factor	q-value
GOCC name	spindle pole	645	105	4	4	6.14	0.19
Amino acid	Y	645	105	4	2	3.07	0.11
Motifs	Pim1 kinase substrate sequence	645	105	16	7	2.69	0.04
Motifs	ATM kinase substrate motif	645	105	17	7	2.53	0.04
Motifs	p70 Ribosomal S6 kinase substrate motif	645	105	13	5	2.36	0.09
Motifs	PAK2 kinase substrate motif	645	105	37	13	2.16	0.02
Motifs	MAPKAPK1 kinase substrate motif	645	105	77	24	1.91	0.00
GOCC slim name	cytoskeleton	645	105	62	19	1.88	0.13
Motifs	PKC epsilon kinase substrate motif	645	105	54	16	1.82	0.03
Motifs	ZIP kinase substrate motif	645	105	38	11	1.78	0.07
Motifs	GSK3 kinase substrate motif	645	105	115	33	1.76	0.00
Amino acid	T	645	105	89	25	1.73	0.00
Motifs	Akt kinase substrate motif	645	105	74	20	1.66	0.03
Motifs	Phosphorylase kinase substrate motif	645	105	46	12	1.60	0.09
Motifs	Chk1 kinase substrate motif	645	105	63	16	1.56	0.07
Motifs	Calmodulin-dependent protein kinase II substrate motif	645	105	213	53	1.53	0.00

Table 6: Over-represented annotation categories from the phosphopeptides that were up-regulated in response to PI3K inhibition in HT29 cells

Category column	Category value	Total size	Selection size	Category size	Intersection size	Enrichment factor	q-value
Motifs	Src kinase substrate motif	675	88	1	1	7.67	0.19
Motifs	JAK2 kinase substrate motif	675	88	1	1	7.67	0.19
Motifs	eIF2 alpha kinase substrate motif	675	88	1	1	7.67	0.20
Charge	5	675	88	1	1	7.67	0.17
KEGG name	Progesterone-mediated oocyte maturation	675	88	5	4	6.14	0.18
KEGG name	Prostate cancer	675	88	6	4	5.11	0.16
Motifs	Doublecortin kinase-1 kinase substrate motif	675	88	3	2	5.11	0.08
KEGG name	Adherens junction	675	88	8	5	4.79	0.10
GOMF name	guanyl ribonucleotide binding	675	88	12	7	4.47	0.06
GOMF name	guanyl nucleotide binding	675	88	12	7	4.47	0.09
GOMF name	GTP binding	675	88	12	7	4.47	0.18
Motifs	CDK4 kinase substrate motif	675	88	4	2	3.84	0.13
GOCC slim name	cell cortex	675	88	11	5	3.49	0.13
Motifs	ATM kinase substrate motif	675	88	18	8	3.41	0.01
Motifs	RAF1 kinase substrate motif	675	88	5	2	3.07	0.17
Motifs	p70 Ribosomal S6 kinase substrate motif	675	88	15	6	3.07	0.02
Motifs	GSK3, Erk1, Erk2 and CDK5 kinase motif	675	88	17	6	2.71	0.04
KEGG name	RNA transport	675	88	23	8	2.67	0.17
Motifs	Calmodulin-dependent protein kinase I substrate motif	675	88	24	8	2.56	0.02
Motifs	Chk1 kinase substrate motif	675	88	68	22	2.48	0.00
Motifs	Calmodulin-dependent protein kinase IV substrate motif	675	88	66	21	2.44	0.00
Motifs	AMP-activated protein kinase 2 substrate motif	675	88	16	5	2.40	0.07
Motifs	AMP-activated protein kinase substrate motif	675	88	29	9	2.38	0.03
Motifs	Calmodulin-dependent protein kinase II substrate motif	675	88	13	4	2.36	0.10
Motifs	Phosphorylase kinase substrate motif	675	88	54	15	2.13	0.01
GOCC slim name	mitochondrion	675	88	40	11	2.11	0.14
Amino acid	T	675	88	96	26	2.08	0.00
Motifs	PKC epsilon kinase substrate motif	675	88	65	16	1.89	0.02
Multiplicity	___3	675	88	31	7	1.73	0.06
Motifs	GSK3 kinase substrate motif	675	88	123	27	1.68	0.01
Motifs	PAK2 kinase substrate motif	675	88	46	10	1.67	0.07
Motifs	DNA dependent Protein kinase substrate motif	675	88	118	25	1.63	0.01
Multiplicity	___2	675	88	222	46	1.59	0.00
Motifs	Pyruvate dehydrogenase kinase substrate motif	675	88	95	19	1.53	0.04
Motifs	CDK kinase substrate motif	675	88	121	24	1.52	0.02

Table 7: Over-represented annotation categories from the phosphopeptides that were up-regulated in response to combined BRAF/PI3K inhibition in HT29 cells

Category column	Category value	Total size	Selection size	Category size	Intersection size	Enrichment factor	q-value
Motifs	Doublecortin kinase-1 kinase substrate motif	609	95	3	2	4.27	0.13
GOMF name	guanyl ribonucleotide binding	609	95	11	7	4.08	0.09
GOMF name	guanyl nucleotide binding	609	95	11	7	4.08	0.13
Motifs	AMP-activated protein kinase substrate motif	609	95	31	15	3.10	0.00
GOBP slim name	neurological system process	609	95	13	6	2.96	0.18
Motifs	p70 Ribosomal S6 kinase substrate motif	609	95	15	6	2.56	0.04
Motifs	Calmodulin-dependent protein kinase II substrate motif	609	95	13	5	2.47	0.07
Motifs	ATM kinase substrate motif	609	95	21	8	2.44	0.03
Motifs	GSK3, Erk1, Erk2 and CDK5 kinase motif	609	95	14	5	2.29	0.09
Motifs	Chk1 kinase substrate motif	609	95	66	23	2.23	0.00
Motifs	HMGCoA Reductase kinase substrate motif	609	95	9	3	2.14	0.18
Motifs	Phosphorylase kinase substrate motif	609	95	51	16	2.01	0.01
Motifs	Pim1 kinase substrate sequence	609	95	16	5	2.00	0.13
Motifs	ZIP kinase substrate motif	609	95	39	12	1.97	0.03
GOBP slim name	death	609	95	46	14	1.95	0.15
GOBP slim name	cell death	609	95	46	14	1.95	0.18
Motifs	PAK2 kinase substrate motif	609	95	40	12	1.92	0.03
Motifs	PKC epsilon kinase substrate motif	609	95	57	17	1.91	0.01
Motifs	Calmodulin-dependent protein kinase IV substrate motif	609	95	61	18	1.89	0.01
Motifs	Calmodulin-dependent protein kinase I substrate motif	609	95	25	7	1.79	0.11
Motifs	AMP-activated protein kinase 2 substrate motif	609	95	15	4	1.71	0.18
Amino acid	T	609	95	83	22	1.70	0.01
Motifs	MAPKAPK1 kinase substrate motif	609	95	70	18	1.65	0.03
Motifs	Calmodulin-dependent protein kinase II substrate motif	609	95	208	52	1.60	0.00
Multiplicity	___2	609	95	165	39	1.52	0.00

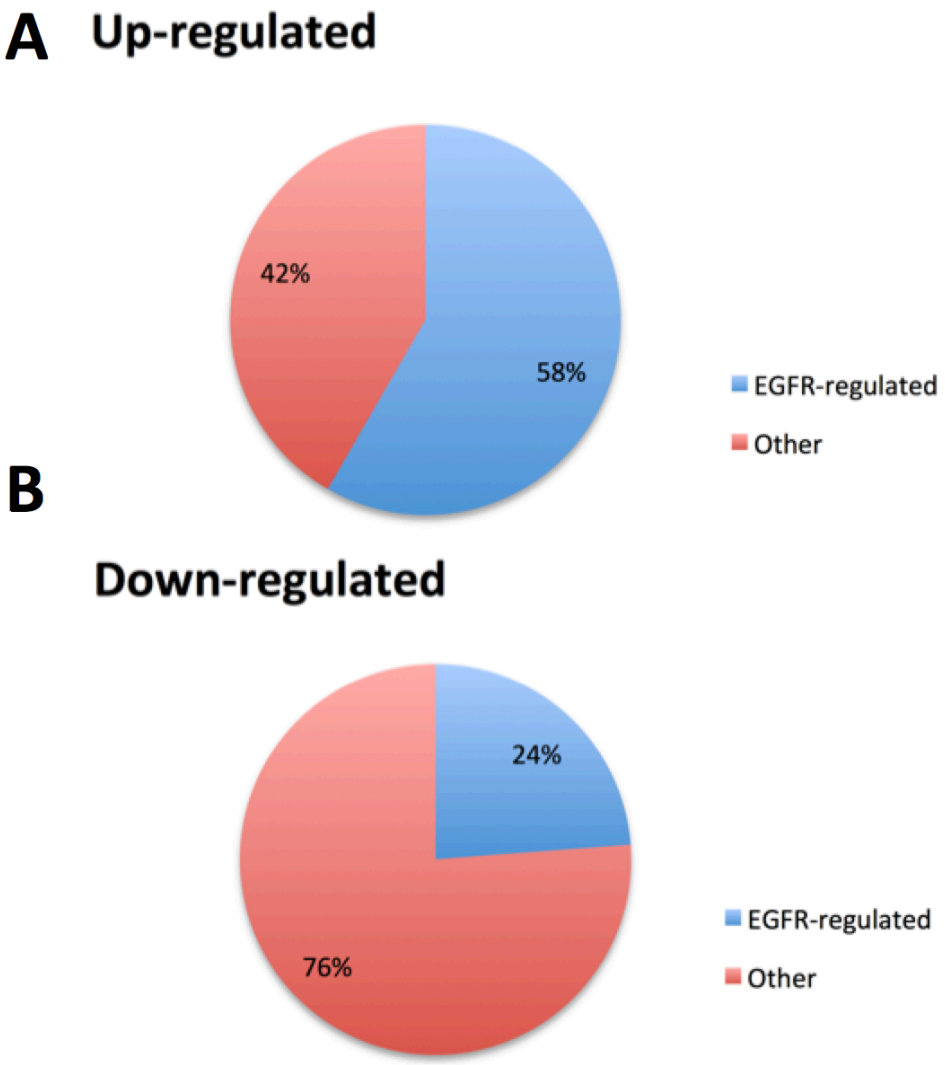

Figure 15: Pie graphs showing the enriched kinases from the HT29 cell data that matched to the phosphopeptides that had been up-regulated (A) or down-regulated (B) following BRAF inhibition. The pie graphs distinguish these kinases based on whether they are regulated by the EGFR or not. Note: Kinases from the MAPK pathway were excluded from this analysis, as this pathway was the target of inhibition.

4 Discussion

The objective of this study was to investigate various inhibition strategies within BRAF-V600E-activated colon cancer cells. The first part of the project involved using cell viability assays to measure the effectiveness of a range of kinase inhibitors. The second part of the project involved using MS-based studies to measure phosphoproteomic changes in BRAF colon cancer cells following exposure to the kinase inhibitors. This phosphoproteomic data was used to hypothesize reasons for the observed efficacy of the different inhibition strategies.

4.1 Investigating protein kinase CK2 inhibitor CX-4945 in BRAF colon cancer cells

The first aim was to measure the effectiveness of CX-4945 (CK2i) in relation to inhibitors with proven efficacy in BRAF colon cancer cells. For the three cell lines with a BRAF mutation, BRAF/protein kinase CK2 inhibition was at least 20% less effective compared to the other combination strategies (Fig 7B, C and D). The ineffectiveness of BRAF/protein kinase CK2 inhibition was even more pronounced in the cell lines with a contiguous PI3K mutation (Fig 7C and D). For example, RKO cells showed a 20% reduction in cell viability in response to BRAF/protein kinase CK2 inhibition compared to an 80% reduction for the cells treated with BRAF/PI3K inhibition (Fig 7D).

These results were surprising considering the effectiveness of BRAF/protein kinase CK2 inhibition in BRAF thyroid and BRAF melanoma cell lines[57]. The effectiveness of the inhibitor combination in these cell lines was explained by an up-regulation of protein kinase CK2 activity in response to BRAF inhibition. As protein kinase CK2 functions in various survival, anti-apoptotic and proliferative pathways such as Wnt signaling and PI3K pathways, its up-regulation is likely an adaptive survival response to BRAF inhibition[68]. In addition, protein kinase CK2 was also shown to have a role in activating the Akt kinase, which exerts its pro-survival effects through the PI3K pathway[69]. Here, Akt is activated by phosphorylation of its Ser129 site, which recruits heat shock protein 90 (HSP90) and reduces phosphatase activity. The reduced phosphatase activity increases the proportion of Akt kinases with an occupied activation site at T308[69].

This would explain why BRAF/protein kinase CK2 inhibition was more effective in the BRAF-mutated Colo205 cells compared to the BRAF/PI3K-mutated HT29 and RKO cells (Fig 7B, C and D). Following protein kinase CK2 inhibition, BRAF-mutated Colo205 cells would have

decreased PI3K pathway output as protein kinase CK2 would no longer be activating Akt, whereas the BRAF/PI3K mutated cells would have continued Akt activation through the PI3K P449T mutation. However, the fact that BRAF/PI3K inhibition was significantly more effective than BRAF/protein kinase CK2 inhibition suggests that the contribution of protein kinase CK2 to PI3K pathway activation is minimal compared to other sources of input such as the EGFR.

Protein kinase CK2 activity could also explain why BRAF/Akt inhibition was more effective than BRAF/PI3K inhibition in the BRAF-mutated Colo205 cells (Fig 7B). Whereas, BRAF/PI3K inhibition was more effective than BRAF/Akt inhibition in the BRAF/PI3K-mutated RKO and HT29 cells (Fig 7C and D). In fact, PI3K/BRAF inhibition was 50% more effective than BRAF/Akt inhibition in the HT29 cells (Fig 7C). These results make sense considering the source of PI3K pathway activation for the two cell types. For the BRAF/PI3K-mutated cells, the majority of PI3K pathway activation comes from the PI3K P449T mutation[70]. In contrast, for the Colo205 cells, a relatively greater proportion of PI3K pathway activation comes from the protein kinase CK2-mediated activation of Akt. Inhibiting PI3K in Colo205 cells does not block protein kinase CK2-mediated activation of Akt, which occurs downstream of PI3K.

Despite variations in the effectiveness of BRAF/protein kinase CK2 inhibition within the different BRAF colon cancer cell lines, the overall effectiveness of the inhibitor combination is minimal compared to its effectiveness within BRAF thyroid and BRAF melanoma cells[57]. The different responses of BRAF thyroid, BRAF melanoma and BRAF colon cancer cells to protein kinase CK2 inhibition highlights the different processes controlling the tumor biology of each cell type.

In spite of promising pre-clinical results, targeted therapies within BRAF colon cancer patients are still limited by the development of acquired resistance[49]. Protein kinase CK2 has been implicated in the formation of multidrug resistance and 'nononcogene addiction' in a variety of cancers, including colon cancer[71]. Whilst protein kinase CK2 inhibition didn't affect the short-term viability of BRAF colon cancer cells in this study (Fig 7), when used in combination with inhibitors that are effective, protein kinase CK2 inhibition may have a role in offsetting the development of acquired resistance.

4.2 Identifying phosphoproteomic changes in BRAF colon cancer cells following inhibition

LFQ mass spectrometry experiments were used to identify changes in the phosphoproteome of BRAF colon cancer cells following exposure to the different inhibition strategies. In response to short-term BRAF inhibition, HT29 cells showed no up-regulation of phosphosubstrates of protein kinase CK2 (Table 5). Rather, there was an over-representation of kinases that function downstream of EGFR (Fig 15). This finding is consistent with previous studies which show that BRAF-inhibited colon cancer cells undergo a rapid feedback activation of EGFR[45,72]. Here, prior to BRAF inhibition, EGFR expression is inhibited via an ERK-mediated negative feedback loop. Upon BRAF inhibition, ERK activity is halted, terminating the negative feedback loop and causing a rapid up-regulation of EGFR kinase expression. As the MAPK pathway is downstream of EGFR, increased EGFR expression eventually leads to reactivation of ERK activity[45]. This reactivation was confirmed by the western blot data, which showed that ERK activity had rebounded after 8 hours of BRAF inhibition in HT29 cells (Fig 8C). Interestingly, this rebound in ERK activity was also observed after 8 hours of PI3K inhibition, highlighting the cross talk between the two pathways[73].

The rapid rebound of ERK activity accounts for why 95% of BRAF colon cancer patients were unresponsive to single-agent BRAF inhibition in a phase I clinical trial, with only 5% showing a partial response[41]. In contrast, 48% of BRAF melanoma patients showed a response to BRAF inhibition, indicating sustained ERK inhibition[39]. These differences in the clinical efficacy of BRAF inhibition between the two cancer types have been largely attributed to greater levels of EGFR within colon cancer cells compared to melanoma cells[74]. In fact, forced EGFR expression in BRAF melanoma cells is sufficient to cause resistance to single-agent BRAF inhibitors[45]. Thus, in response to BRAF inhibition, BRAF colon cancer cells show increased EGFR activity rather than increased protein kinase CK2 activity.

4.3 Combined BRAF/PI3K inhibition is effective in BRAF colon cancer cells

BRAF thyroid cancer cells show both high levels of EGFR expression and up-regulated protein kinase CK2 activity in response to BRAF inhibition, showing that these responses don't have to be independent of each other[57]. In contrast, BRAF colon cancer cells respond to BRAF inhibition predominantly through increased EGFR expression, with minimal reliance on alternative pro-survival pathways[75]. This reliance on survival pathways downstream of EGFR explains the effectiveness of the BRAF/PI3K inhibitor combination, which showed >60%

growth inhibition for all three BRAF-mutated cell lines but <20% growth inhibition for the BRAF wild-type cell line (Fig 7A, B, C and D). Furthermore, the DAVID functional analysis of the phosphopeptides that had been up-regulated in response to BRAF/PI3K inhibition revealed that 19.4% of the phosphopeptides fell under the 'regulation of programmed cell death' GO annotation category (Supplementary table 10). Likewise, the Fisher exact test within Perseus revealed that this same set of phosphopeptides had a 1.95-fold enrichment of the 'cell death' GO annotation category.

The BRAF/PI3K inhibitor combination has already been shown to be effective in a range of colon cancer cell lines, especially cell lines with a PTEN deletion or a PI3K gain-of-function mutation[76]. Cell lines with these mutations are less sensitive to single-agent BRAF inhibition. In fact, knockdown of PTEN expression in sensitive colon cancer cell lines increased their resistance to BRAF inhibition[12]. Combined BRAF/PI3K inhibition was able to overcome BRAF inhibitor resistance in these cell lines[12]. In a later study, combined PI3K/BRAF inhibition was effective at treating mice with xenografts from human colon cancer cell lines, including cell lines with PTEN and PI3K mutations[10]. Considering that 13% of BRAF colon cancer patients harbor a PI3K mutation and 22% have a PTEN deletion, it is surprising that there have been no clinical trials involving combined BRAF/PI3K inhibition for BRAF colon cancer patients[77]. Although, a clinical trial comparing the BRAF inhibitor encorafenib and cetuximab, with and without the PI3K inhibitor alpelisib is anticipated to begin soon[52].

4.4 Paradoxical activation of BRAF wild-type cells in response to BRAF inhibition

BRAF wild-type cells are known to show paradoxical activation of ERK activity in response to BRAF inhibition[78]. However, the western blot data shows that ERK activity steadily declined over the 24-hour time period in the BRAF wild-type SW480 cells (Fig 8A). A possible explanation is that ERK activity did initially increase but was not detected due to the limited number of time points. This increased ERK activity would have increased the strength of the negative feedback loops acting on the RTK's that regulate MAPK pathway output, such as the EGFR. As a result, ERK activity steadily declined. This explanation is supported by a model of the adaptive response of BRAF cancer cells to BRAF inhibition[16]. Here, the cellular response to BRAF inhibition cycles through phases of high ERK activity/strong ERK-mediated negative feedback and low ERK activity/weak negative feedback until equilibrium is reached.

Of note, in the same way that ERK activity rebounded after only 8 hours of BRAF inhibition in BRAF-mutated cells, paradoxical activation of ERK lasted only 8 hours in BRAF wild-type colon cancer cells, which is indicated by reduced ERK levels at the 8 hour time-point (Fig 8A and C). In contrast, BRAF inhibition in BRAF-mutated melanoma cells results in sustained periods of ERK inhibition before any rebound of ERK activity is observed[79]. Likewise, paradoxical activation lasts for extended periods of time in BRAF wild-type melanoma cells[80]. Both of these processes are influenced by the EGFR[81]. For example, the initial paradoxical activation of ERK results in negative feedback inhibition of EGFR. Once inhibited, the EGFR's contribution to MAPK pathway activation is diminished, resulting in less RAS-mediated RAF dimerization and a greater proportion of RAF kinases functioning as inhibitor-sensitive monomers. As a result, ERK levels steadily decline. However, as already mentioned, BRAF melanoma cells have lower levels of EGFR expression and undergo MAPK pathway activation through alternative RTK's that are not subject to the same degree of ERK-mediated negative feedback, which accounts for the sustained activation of ERK in BRAF wild-type cells[82]. The fact that the 'paradoxical activation' phenomenon was described in BRAF melanoma cells explains why the Western blot data differs from what was expected.

4.5 Changes in the regulation of phosphosites in response to inhibitor treatments

Whilst the majority of phosphosites were either all up-regulated or all down-regulated in comparison to the control, a number of phosphosites were differnetailly regulated between the different treatment groups. For example, phosphosite T646 within multidrug-resistance protein 4 (UniProt: O15439) and phosphosite S2559 chromodomain-helicase DNA binding protein 7 (UniProt: QP92D1) were up-regulated in response to dabrafenib but down-regulated in response to the GDC0941 and GDC + Dab inhibitor treatments (Fig 13). Multidrug-resistance protein 4 is an ATP-binding cassette transporter which regulates levels of physiological substrates such as lipids[83]. Some ABC transporters have a role in removing xenobiotics from cells. In fact, up-regulation of ABC transporters is one of the most common mechanisms for acquired resistance to chemotherapeutics[83]. Recently, it was shown that the PI3K pathway regulates the activity of ABC transporters in glioma tumor stem-like cells[84]. Here, treatment with the PI3K inhibitor GDC0941 reduced the activity of ABC transporter G2. The fact that the PI3K pathway regulates ABC transporter activity explains why phosphosites from multidrug-resistance protein 4 were differentially expressed between the different inhibitor treatments. For the dabrafenib treatment, a rise in cellular xenobiotic levels would

have increased ABC transporter expression whereas inhibiting the PI3K pathway in the GDC0941 treatments would have decreased its expression.

4.6 Limitations

One of the main limitations of the project was the relatively low number of phosphopeptides that were identified for the Colo205 samples. Only 2148 phosphopeptides were identified across the 18 samples that were run. This number was reduced to 372 phosphopeptides for the ANOVA analysis, as the data was filtered to ensure that each treatment group had valid values for at least 2/3 replicates. The low number of phosphopeptides identified could be attributed to the complexity and dynamic range of the phosphoproteome, which makes achieving high coverage difficult[85]. Methods to reduce this complexity include using fractionation techniques such as SCX, HILIC and ERLIC to increase the efficiency of the phosphopeptide enrichment step[86]. Whilst pre-fractionation techniques could have increased phosphoproteome coverage, these methods require large amounts of starting material and each fraction requires its own preparation and analysis, which was not practical for this time restricted project.

Another method to increase phosphoproteome coverage would be the use of longer LC columns to increase phosphopeptide separation[86]. In a recent study, it was shown that longer separation columns resulted in more peptide identifications[87]. Here, shotgun proteomics experiments were conducted on A375 cancer cells using either a 15cm, 25cm or 50cm separation column. The 50cm column produced more peptide identifications at each gradient length tested. For example, approximately 43000 peptides were identified using a 50cm column with a 3-hour gradient compared to 23000 peptides for the 15cm column[87]. In this project, the relatively low peptide separation achieved using a 10cm column would have contributed to the low number of phosphopeptides identified. Interestingly, almost twice as many phosphopeptides were identified for the HT29 samples compared to the Colo205 samples (Table 2 and 3). This difference is likely a result of the Colo205 samples being run before the Q-Exactive mass spectrometer was serviced and the HT29 samples being run after the machine had been serviced.

Another limitation was the relatively high coefficient of variation (CV) for some of the treatment groups. For example, for the Colo205 cells treated with combined dabrafenib and GDC0941 inhibition, the CV was 57.6% (Table 3). The low number of phosphopeptides

identified for the Colo205 cells combined with the high CV's of some of the treatment groups limited the usefulness of much of this data. An explanation for the relatively high CV's is that LFQ was used. Whilst LFQ is inexpensive, its limitation is that each sample requires its own separate MS analysis, which increases quantitation error due to inconsistent sample preparation[60]. Chemical labeling methods such as SILAC and iTRAQ could be used to reduce the CV by allowing samples to be pooled.

In contrast to the Colo205 cell data, the HT29 cell data had lower CV's and higher phosphopeptide identifications, making its bioinformatics analysis more useful. However, for many of the phosphopeptides that were considered interesting, there was no information available on the function of the phosphorylation sites. This represents a limitation that is common to most phosphoproteomics experiments[86]. The majority of phosphoproteomics experiments aim to increase understanding of cellular signaling. However, even with large datasets, these experiments can be limited due to the lack of characterization of many of the phosphorylation sites[86].

4.7 Future directions

Targeted therapies with sustainable anti-tumor effects are desperately needed for the treatment of BRAF colon cancer. Whilst BRAF/protein kinase CK2 inhibition showed limited effectiveness in BRAF colon cancer cells, many recent studies offer promise that more effective treatment options may soon be available. For example, pan-RAF inhibitors have recently been developed that inhibit BRAF V600E, CRAF and SRC family kinases (SFK's)[88]. As RTK's such as the EGFR signal through SFK's, inhibiting SFK's is predicted to dampen EGFR-mediated reactivation of the MAPK pathway. In addition, it was shown that colon cancer cells with acquired resistance to EGFR-targeted therapies had increased SFK phosphorylation[1]. In fact, combining the SFK inhibitor PP2 with an EGFR inhibitor was shown to induce apoptosis in the resistant cells[1].

Furthermore, resistance to current inhibition strategies is often mediated via the formation of inhibitor-resistant RAF dimers such as BRAF V600E-CRAF[16]. Pan-RAF inhibitors that inhibit CRAF will prevent much of the dimer-mediated activation of MEK. Indeed, it has been shown that mutant NRAS and KRAS signal exclusively through CRAF[89]. Thus, pan-RAF inhibitors are predicted to be active against BRAF tumors that develop RAS alterations. Alterations such as

mutant KRAS, amplified KRAS and amplified CRAF have already been identified as mechanisms of acquired resistance in BRAF colon cancer patients[44].

Additionally, pan-RAF inhibitors have demonstrated increased activity against BRAF colon cancer cells compared to vemurafenib and dabrafenib[88]. Clinical trials of pan-RAF inhibitors are due to start in 2015[88]. Interestingly, the SRC kinase substrate motif was enriched 7.67-fold for the phosphopeptides that were up-regulated in response to PI3K inhibition (Table 6). Thus, it is likely that increased SRC kinase activity is a survival response to PI3K inhibition that functions to re-activate EGFR and MAPK pathways. These findings provide rationale that combinations of pan-RAF, EGFR and SRC kinase inhibitors could be effective treatment options for BRAF colon cancer patients.

Another promising treatment option involves targeting the RAF dimerization interface[90]. Much of the resistance attributed to MAPK pathway reactivation is due to the formation of inhibitor resistant RAF dimers. Preventing this dimerization may be an effective treatment option. Recently, a peptide was developed that blocks RAF dimerization[90]. However, developing a peptide with enough potency to be used in clinical trials remains a challenge. Preventing dimers from activating MEK may also be achieved by developing more selective BRAF/CRAF inhibitors[16]. Such inhibitors may be able to bind to both partners of the RAF dimer, inactivating the entire complex. However, both of these strategies have limitations. Firstly, numerous resistance mechanisms have been identified in BRAF cancer patients that abrogate RAF dimerization such as BRAF splice variants, activating MEK mutations and PI3K pathway alterations[79]. In addition, such compounds will be active in both BRAF V600E and BRAF wild-type cells, resulting in smaller therapeutic indexes[16].

Introducing ERK inhibitors into combination strategies could also be an effective treatment option for BRAF colon cancer patients[44]. Colon cancer cell lines that are resistant to BRAF/MEK and BRAF/EGFR inhibitor combinations remained sensitive to the ERK inhibitor VX-11E[44]. These cell lines contained either a KRAS amplification, BRAF amplification or an activating MEK1 mutation; the three mechanisms of acquired resistance identified in BRAF colon cancer patients to date[44]. There are numerous ERK inhibitors that are currently about to enter or have entered early phase clinical trials[91]. Inhibitors have been developed for virtually every protein within the MAPK cascade including BRAF, CRAF and MEK, which are all kinases. However, inhibitors are yet to be developed for RAS GTPase, which has been classified as

'undruggable'[92]. As RAS is responsible for activating BRAF and CRAF and catalyzing their dimerization, developing RAS inhibitors may revolutionize the treatment of BRAF colon cancer and many other cancer types.

4.8 Conclusion

Targeted therapies need to produce anti-tumor effects for over 10 months if they are to replace cytotoxic chemotherapy treatments for BRAF colon cancer patients. To date, the most effective targeted therapy has been a BRAF/EGFR inhibitor combination that produced an overall survival rate of 7.6 months in BRAF colon cancer patients. Unfortunately, the initial therapeutic effects of targeted therapies are offset by the development of acquired resistance. As understanding of the mechanisms of acquired resistance increase, more effective inhibitor and inhibitor combinations should be developed. Developments such as pan-RAF inhibitors, ERK inhibitors, dimerization interface peptides, more selective BRAF and PI3K inhibitors and more personalized combination strategies have the potential to offset or prevent the formation of drug resistance. In this project, the effectiveness of a novel targeted therapy involving a BRAF/Protein kinase CK2 inhibitor combination was evaluated in an effort to develop a more sustainable targeted therapy. Whilst this combination was not as effective as existing therapies, the study provided useful biological insight into how the phosphoproteome of BRAF colon cancer cells responds to various kinase inhibitors. For example, the up-regulation of SRC kinase activity in response to PI3K inhibition provides rationale for the evaluation of different combinations of PI3K/EGFR/pan-RAF inhibitors in BRAF colon cancer cells.

References:

1 Van Emburgh, B. O., Sartore-Bianchi, A., Di Nicolantonio, F., Siena, S. & Bardelli, A. Acquired resistance to EGFR-targeted therapies in colorectal cancer. *Molecular oncology* **8**, 1084-1094 (2014).

2 Goodwin, M. Cancer incidence projections Australia, 2011 to 2020. *Australian Institute of Health and Welfare*, (2012).

3 Siegel, R., Ma, J., Zou, Z. & Jemal, A. Cancer statistics, 2014. *CA: a cancer journal for clinicians* **64**, 9-29 (2014).

4 Ciombor, K. K., Wu, C. & Goldberg, R. M. Recent therapeutic advances in the treatment of colorectal cancer. *Annual review of medicine* **66**, 83-95 (2015).

5 Heinemann, V. *et al.* FOLFIRI plus cetuximab versus FOLFIRI plus bevacizumab as first-line treatment for patients with metastatic colorectal cancer (FIRE-3): a randomised, open-label, phase 3 trial. *The Lancet Oncology* **15**, 1065-1075 (2014).

6 Douillard, J. *et al.* Irinotecan combined with fluorouracil compared with fluorouracil alone as first-line treatment for metastatic colorectal cancer: a multicentre randomised trial. *The Lancet* **355**, 1041-1047 (2000).

7 Fearon, E. R. & Vogelstein, B. A genetic model for colorectal tumorigenesis. *Cell* **61**, 759-767 (1990).

8 Cantwell-Dorris, E. R., O'Leary, J. J. & Sheils, O. M. BRAFV600E: implications for carcinogenesis and molecular therapy. *Molecular cancer therapeutics* **10**, 385-394 (2011).

9 Leggett, B. & Whitehall, V. Role of the serrated pathway in colorectal cancer pathogenesis. *Gastroenterology* **138**, 2088-2100 (2010).

10 Rad, R. *et al.* A genetic progression model of Braf V600E-induced intestinal tumorigenesis reveals targets for therapeutic intervention. *Cancer cell* **24**, 15-29 (2013).

11 Samowitz, W. S. *et al.* Poor survival associated with the BRAF V600E mutation in microsatellite-stable colon cancers. *Cancer research* **65**, 6063-6069 (2005).

12 Mao, M. *et al.* Resistance to BRAF inhibition in BRAF-mutant colon cancer can be overcome with PI3K inhibition or demethylating agents. *Clinical cancer research* **19**, 657-667 (2013).

13 Roth, A. D. *et al.* Prognostic role of KRAS and BRAF in stage II and III resected colon cancer: results of the translational study on the PETACC-3, EORTC 40993, SAKK 60-00 trial. *Journal of Clinical Oncology* **28**, 466-474 (2010).

14 Roskoski, R. RAF protein-serine/threonine kinases: structure and regulation. *Biochemical and biophysical research communications* **399**, 313-317 (2010).

15 De Luca, A., Maiello, M. R., D'Alessio, A., Pergameno, M. & Normanno, N. The RAS/RAF/MEK/ERK and the PI3K/AKT signalling pathways: role in cancer pathogenesis and implications for therapeutic approaches. *Expert opinion on therapeutic targets* **16**, S17-S27 (2012).

16 Lito, P., Rosen, N. & Solit, D. B. Tumor adaptation and resistance to RAF inhibitors. *Nature medicine* **19**, 1401-1409 (2013).

17 Weber, C. K., Slupsky, J. R., Kalmes, H. A. & Rapp, U. R. Active Ras induces heterodimerization of cRaf and BRaf. *Cancer research* **61**, 3595-3598 (2001).

18 Britten, C. D. PI3K and MEK inhibitor combinations: examining the evidence in selected tumor types. *Cancer chemotherapy and pharmacology* **71**, 1395-1409 (2013).

19 Shin, S.-Y. *et al.* Positive-and negative-feedback regulations coordinate the dynamic behavior of the Ras-Raf-MEK-ERK signal transduction pathway. *Journal of cell science* **122**, 425-435 (2009).

20 Pratilas, C. A. & Solit, D. B. Targeting the mitogen-activated protein kinase pathway: physiological feedback and drug response. *Clinical Cancer Research* **16**, 3329-3334 (2010).
21 Rapp, U. *et al.* Structure and biological activity of v-raf, a unique oncogene transduced by a retrovirus. *Proceedings of the National Academy of Sciences* **80**, 4218-4222 (1983).
22 Davies, H. *et al.* Mutations of the BRAF gene in human cancer. *Nature* **417**, 949-954 (2002).
23 Blachly, J. S. *et al.* Cotreatment of Hairy Cell Leukemia and Melanoma With the BRAF Inhibitor Dabrafenib. *Journal of the National Comprehensive Cancer Network* **13**, 9-13 (2015).
24 Nucera, C., Goldfarb, M., Hodin, R. & Parangi, S. Role of B-Raf V600E in differentiated thyroid cancer and preclinical validation of compounds against B-Raf V600E. *Biochimica et Biophysica Acta (BBA)-Reviews on Cancer* **1795**, 152-161 (2009).
25 Thevakumaran, N. *et al.* Crystal structure of a BRAF kinase domain monomer explains basis for allosteric regulation. *Nature Structural & Molecular Biology* (2014).
26 Wan, P. T. *et al.* Mechanism of activation of the RAF-ERK signaling pathway by oncogenic mutations of B-RAF. *Cell* **116**, 855-867 (2004).
27 Eichhorn, P. J., Creyghton, M. P. & Bernards, R. Protein phosphatase 2A regulatory subunits and cancer. *Biochimica et Biophysica Acta (BBA)-Reviews on Cancer* **1795**, 1-15 (2009).
28 Lito, P. *et al.* Relief of profound feedback inhibition of mitogenic signaling by RAF inhibitors attenuates their activity in BRAFV600E melanomas. *Cancer cell* **22**, 668-682 (2012).
29 Poulikakos, P. I. *et al.* RAF inhibitor resistance is mediated by dimerization of aberrantly spliced BRAF (V600E). *Nature* **480**, 387-390 (2011).
30 Belden, S. & Flaherty, K. T. MEK and RAF inhibitors for BRAF-mutated cancers. *Expert reviews in molecular medicine* **14**, e17 (2012).
31 Wilhelm, S. M. *et al.* BAY 43-9006 exhibits broad spectrum oral antitumor activity and targets the RAF/MEK/ERK pathway and receptor tyrosine kinases involved in tumor progression and angiogenesis. *Cancer research* **64**, 7099-7109 (2004).
32 Sala, E. *et al.* BRAF silencing by short hairpin RNA or chemical blockade by PLX4032 leads to different responses in melanoma and thyroid carcinoma cells. *Molecular Cancer Research* **6**, 751-759 (2008).
33 Tsai, J. *et al.* Discovery of a selective inhibitor of oncogenic B-Raf kinase with potent antimelanoma activity. *Proceedings of the National Academy of Sciences* **105**, 3041-3046 (2008).
34 Mittapalli, R. K., Vaidhyanathan, S., Dudek, A. Z. & Elmquist, W. F. Mechanisms limiting distribution of the BRAFV600E inhibitor dabrafenib to the brain: implications for the treatment of melanoma brain metastases. *Journal of Pharmacology and Experimental Therapeutics*, jpet. 112.201475 (2012).
35 Bollag, G. *et al.* Clinical efficacy of a RAF inhibitor needs broad target blockade in BRAF-mutant melanoma. *Nature* **467**, 596-599 (2010).
36 Poulikakos, P. I., Zhang, C., Bollag, G., Shokat, K. M. & Rosen, N. RAF inhibitors transactivate RAF dimers and ERK signalling in cells with wild-type BRAF. *Nature* **464**, 427-430 (2010).
37 Heidorn, S. J. *et al.* Kinase-dead BRAF and oncogenic RAS cooperate to drive tumor progression through CRAF. *Cell* **140**, 209-221 (2010).
38 Holderfield, M., Nagel, T. & Stuart, D. Mechanism and consequences of RAF kinase activation by small-molecule inhibitors. *British journal of cancer* (2014).
39 Chapman, P. B. *et al.* Improved survival with vemurafenib in melanoma with BRAF V600E mutation. *New England Journal of Medicine* **364**, 2507-2516 (2011).

40 Hall, R. D. & Kudchadkar, R. R. BRAF mutations: signaling, epidemiology, and clinical experience in multiple malignancies. *Cancer Control* **21**, 221-230 (2014).
41 Kopetz, S. *et al.* PLX4032 in metastatic colorectal cancer patients with mutant BRAF tumors. *ASCO Annual Meeting Proceedings,* **28,** 3534 (2010).
42 Falchook, G. S. *et al.* Dabrafenib in patients with melanoma, untreated brain metastases, and other solid tumours: a phase 1 dose-escalation trial. *The Lancet* **379**, 1893-1901 (2012).
43 Joseph, E. W. *et al.* The RAF inhibitor PLX4032 inhibits ERK signaling and tumor cell proliferation in a V600E BRAF-selective manner. *Proceedings of the National Academy of Sciences*, 201008990 (2010).
44 Ahronian, L. G. *et al.* Clinical acquired resistance to RAF inhibitor combinations in BRAF-mutant colorectal cancer through MAPK pathway alterations. *Cancer discovery*, CD-14-1518 (2015).
45 Prahallad, A. *et al.* Unresponsiveness of colon cancer to BRAF (V600E) inhibition through feedback activation of EGFR. *Nature* **483**, 100-103 (2012).
46 Corcoran, R. B. *et al.* Phase 1-2 trial of the BRAF inhibitor danrafenib (D) plus MEK inhibitor tranetinib (T) in BRAF V600 mutant colorectal cancer (CRC): updated efficacy and biomarker analysis. *ASCO Annual Meeting Proceedings* **32**, 15 (2014).
47 Flaherty, K. T. *et al.* Combined BRAF and MEK inhibition in melanoma with BRAF V600 mutations. *New England Journal of Medicine* **367**, 1694-1703 (2012).
48 Turke, A. B. *et al.* MEK inhibition leads to PI3K/AKT activation by relieving a negative feedback on ERBB receptors. *Cancer research* **72**, 3228-3237 (2012).
49 Ahronian, L. G. *et al.* Clinical acquired resistance to RAF inhibitor combinations in BRAF-mutant colorectal cancer through MAPK pathway alterations. *Cancer discovery* **5**, 358-367 (2015).
50 Yaeger, R. *et al.* Pilot Trial of Combined BRAF and EGFR Inhibition in BRAF Mutant Metastatic Colorectal Cancer Patients. *Clinical Cancer Research*, **2779,** 2014 (2015).
51 Tabernero, J. *et al.* VE-BASKET, a Simon 2-stage adaptive design, phase II, histology-independent study in nonmelanoma solid tumors harboring BRAF V600 mutations (V600m): Activity of vemurafenib (VEM) with or without cetuximab (CTX) in colorectal cancer (CRC). *Journal of Clinical Oncology* **32** (2014).
52 Tabernero, J. *et al.* 11LBA Phase I study of the selective BRAFV600 inhibitor encorafenib (LGX818) combined with cetuximab and with or without the α-specific PI3K inhibitor alpelisib (BYL719) in patients with advanced BRAF mutant colorectal cancer. *European Journal of Cancer* **50**, 199 (2014).
53 Bendell, J. *et al.* Efficacy and tolerability in an open-label phase I/II study of MEK inhibitor trametinib (T), BRAF inhibitor dabrafenib (D), and anti-EGFR antibody panitumumab (P) in combination in patients (pts) with BRAF V600E mutated colorectal cancer (CRC). *Journal of Clinical Oncology* **32**, 3515 (2014).
54 Bokemeyer, C. *et al.* Addition of cetuximab to chemotherapy as first-line treatment for KRAS wild-type metastatic colorectal cancer: pooled analysis of the CRYSTAL and OPUS randomised clinical trials. *European Journal of Cancer* **48**, 1466-1475 (2012).
55 Bromberg-White, J. L., Andersen, N. J. & Duesbery, N. S. MEK genomics in development and disease. *Briefings in functional genomics* **11**, 300-310 (2012).
56 Guerra, B. & Issinger, O. G. Protein kinase CK2 and its role in cellular proliferation, development and pathology. *Electrophoresis* **20**, 391-408 (1999).
57 Parker, R., Clifton-Bligh, R. & Molloy, M. P. Phosphoproteomics of MAPK inhibition in BRAF-mutated cells and a role for the lethal synergism of dual BRAF and CK2 inhibition. *Molecular cancer therapeutics* **13**, 1894-1906 (2014).

58 Siddiqui-Jain, A. *et al.* CX-4945, an orally bioavailable selective inhibitor of protein kinase CK2, inhibits prosurvival and angiogenic signaling and exhibits antitumor efficacy. *Cancer research* **70**, 10288-10298 (2010).
59 Bliesath, J. *et al.* Combined inhibition of EGFR and CK2 augments the attenuation of PI3K-Akt-mTOR signaling and the killing of cancer cells. *Cancer letters* **322**, 113-118 (2012).
60 Nita-Lazar, A., Saito-Benz, H. & White, F. M. Quantitative phosphoproteomics by mass spectrometry: past, present, and future. *Proteomics* **8**, 4433 (2008).
61 Rigbolt, K. T. & Blagoev, B. Quantitative phosphoproteomics to characterize signaling networks. *Seminars in cell & developmental biology* **23,** 863-871 (2012).
62 Beltran, L. & Cutillas, P. R. Advances in phosphopeptide enrichment techniques for phosphoproteomics. *Amino acids* **43**, 1009-1024 (2012).
63 Cox, J. *et al.* Accurate proteome-wide label-free quantification by delayed normalization and maximal peptide ratio extraction, termed MaxLFQ. *Molecular & Cellular Proteomics* **13**, 2513-2526 (2014).
64 Cox, J. & Mann, M. 1D and 2D annotation enrichment: a statistical method integrating quantitative proteomics with complementary high-throughput data. *BMC bioinformatics* **13**, S12 (2012).
65 Huang, D. W., Sherman, B. T. & Lempicki, R. A. Systematic and integrative analysis of large gene lists using DAVID bioinformatics resources. *Nature protocols* **4**, 44-57 (2008).
66 Huang, D. W., Sherman, B. T. & Lempicki, R. A. Bioinformatics enrichment tools: paths toward the comprehensive functional analysis of large gene lists. *Nucleic acids research* **37**, 1-13 (2009).
67 Hornbeck, P. V. *et al.* PhosphoSitePlus, 2014: mutations, PTMs and recalibrations. *Nucleic acids research* **43**, D512-D520 (2015).
68 Gray, G. K., McFarland, B. C., Rowse, A. L., Gibson, S. A. & Benveniste, E. N. Therapeutic CK2 inhibition attenuates diverse prosurvival signaling cascades and decreases cell viability in human breast cancer cells. *Oncotarget* **5**, 6484 (2014).
69 Di Maira, G., Brustolon, F., Pinna, L. A. & Ruzzene, M. Dephosphorylation and inactivation of Akt/PKB is counteracted by protein kinase CK2 in HEK 293T cells. *Cellular and molecular life sciences* **66**, 3363-3373 (2009).
70 Dan, S. *et al.* Correlating phosphatidylinositol 3-kinase inhibitor efficacy with signaling pathway status: in silico and biological evaluations. *Cancer research* **70**, 4982-4994 (2010).
71 Ruzzene, M. & Pinna, L. A. Addiction to protein kinase CK2: a common denominator of diverse cancer cells? *Biochimica et Biophysica Acta (BBA)-Proteins and Proteomics* **1804**, 499-504 (2010).
72 Ahronian, L. G. & Corcoran, R. B. Effective MAPK inhibition is critical for therapeutic responses in colorectal cancer with BRAF mutations. *Molecular & Cellular Oncology*, 00-00 (2015).
73 Aksamitiene, E., Kiyatkin, A. B. & Kholodenko, B. N. Cross-talk between mitogenic Ras/MAPK and survival PI3K/Akt pathways: a fine balance. *Biochemical Society Transactions* **40, 139-146** (2012).
74 Yaeger, R. *et al.* Pilot trial of combined BRAF and EGFR inhibition in BRAF-mutant metastatic colorectal cancer patients. *Clinical Cancer Research* **21**, 1313-1320 (2015).
75 Corcoran, R. B. *et al.* EGFR-mediated reactivation of MAPK signaling contributes to insensitivity of BRAF-mutant colorectal cancers to RAF inhibition with vemurafenib. *Cancer discovery* **2**, 227-235 (2012).

76 Yang, H. *et al.* Preclinical combinations of vemurafenib, a selective BRAF inhibitor, with other targeted therapies in BRAFV600E colorectal cancer models. *Cancer Research* **72**, 2156-2156 (2012).
77 Bamford, S. *et al.* The COSMIC (Catalogue of Somatic Mutations in Cancer) database and website. *British journal of cancer* **91**, 355-358 (2004).
78 Joseph, E. W. *et al.* The RAF inhibitor PLX4032 inhibits ERK signaling and tumor cell proliferation in a V600E BRAF-selective manner. *Proceedings of the National Academy of Sciences* **107**, 14903-14908 (2010).
79 Alcala, A. M. & Flaherty, K. T. BRAF inhibitors for the treatment of metastatic melanoma: clinical trials and mechanisms of resistance. *Clinical Cancer Research* **18**, 33-39 (2012).
80 Chapman, P. B., Solit, D. B. & Rosen, N. Combination of RAF and MEK Inhibition for the Treatment of BRAF-Mutated Melanoma: Feedback Is Not Encouraged. *Cancer cell* **26**, 603-604 (2014).
81 Solit, D. B. & Janne, P. A. Translational medicine: Primed for resistance. *nature* **483**, 44-45 (2012).
82 Sun, C. *et al.* Reversible and adaptive resistance to BRAF (V600E) inhibition in melanoma. *Nature* **508**, 118-122 (2014).
83 Wu, C.-P. & Ambudkar, S. V. The pharmacological impact of ATP-binding cassette drug transporters on vemurafenib-based therapy. *Acta Pharmaceutica Sinica B* **4**, 105-111 (2014).
84 Bleau, A.M. *et al.* PTEN/PI3K/Akt pathway regulates the side population phenotype and ABCG2 activity in glioma tumor stem-like cells. *Cell stem cell* **4**, 226-235 (2009).
85 Dunn, J. D., Reid, G. E. & Bruening, M. L. Techniques for phosphopeptide enrichment prior to analysis by mass spectrometry. *Mass spectrometry reviews* **29**, 29-54 (2010).
86 Han, G., Ye, M. & Zou, H. Development of phosphopeptide enrichment techniques for phosphoproteome analysis. *Analyst* **133**, 1128-1138 (2008).
87 Pirmoradian, M. *et al.* Rapid and deep human proteome analysis by single-dimension shotgun proteomics. *Molecular & Cellular Proteomics* **12**, 3330-3338 (2013).
88 Girotti, M. R. *et al.* Paradox-Breaking RAF Inhibitors that Also Target SRC Are Effective in Drug-Resistant BRAF Mutant Melanoma. *Cancer cell* **27**, 85-96 (2015).
89 Rebocho, A. P. & Marais, R. New insight puts CRAF in sight as a therapeutic target. *Cancer discovery* **1**, 98-99 (2011).
90 Freeman, A. K., Ritt, D. A. & Morrison, D. K. Effects of Raf dimerization and its inhibition on normal and disease-associated Raf signaling. *Molecular cell* **49**, 751-758 (2013).
91 Morris, E. J. *et al.* Discovery of a novel ERK inhibitor with activity in models of acquired resistance to BRAF and MEK inhibitors. *Cancer discovery* **3**, 742-750 (2013).
92 Downward, J. Targeting RAF: trials and tribulations. *Nature medicine* **17**, 286-288 (2011).

Supplementary material:

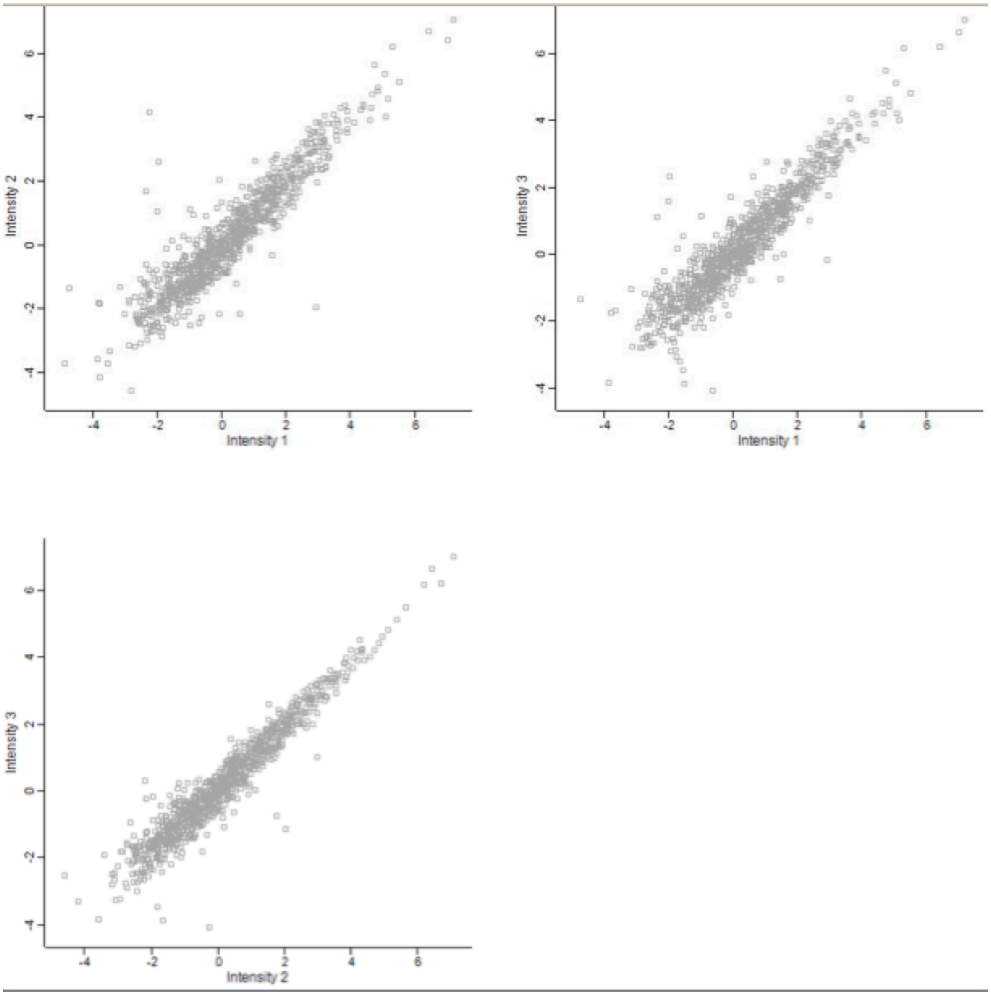

Supplementary figure 1: Scatterplots of the three control replicates from the HT29 cell sample, showing strong correlation. Intensity 1, 2 and 3 correspond to control replicate 1, 2 and 3.

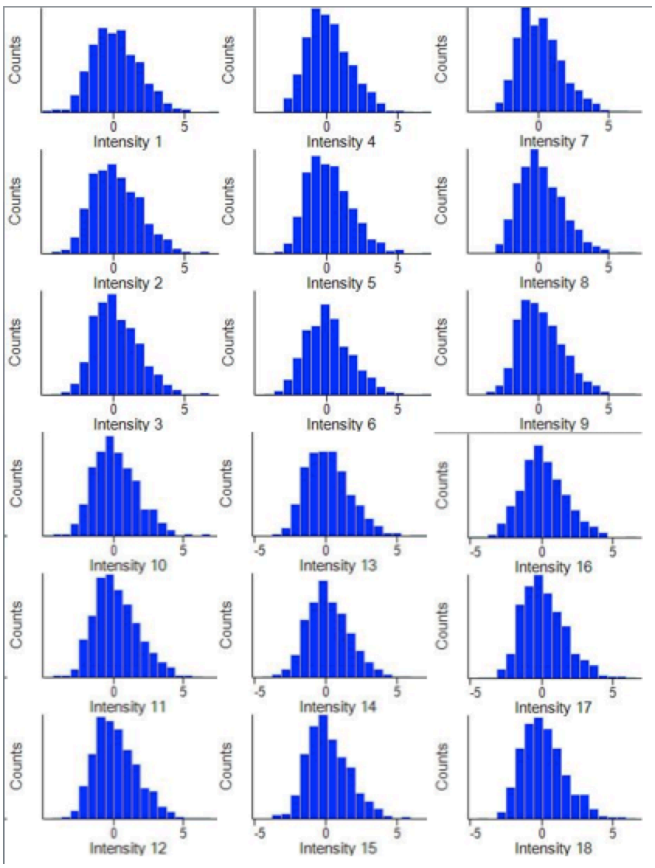

Supplementary figure 2: Histograms of the 18 HT29 cell samples showing that the data was normally distributed before being analysed. Intensity 1-18 corresponds to the control, dabrafenib, GDC0941, CX-4945, Dab+GDC and Dab+CX samples, which were run in triplicates.

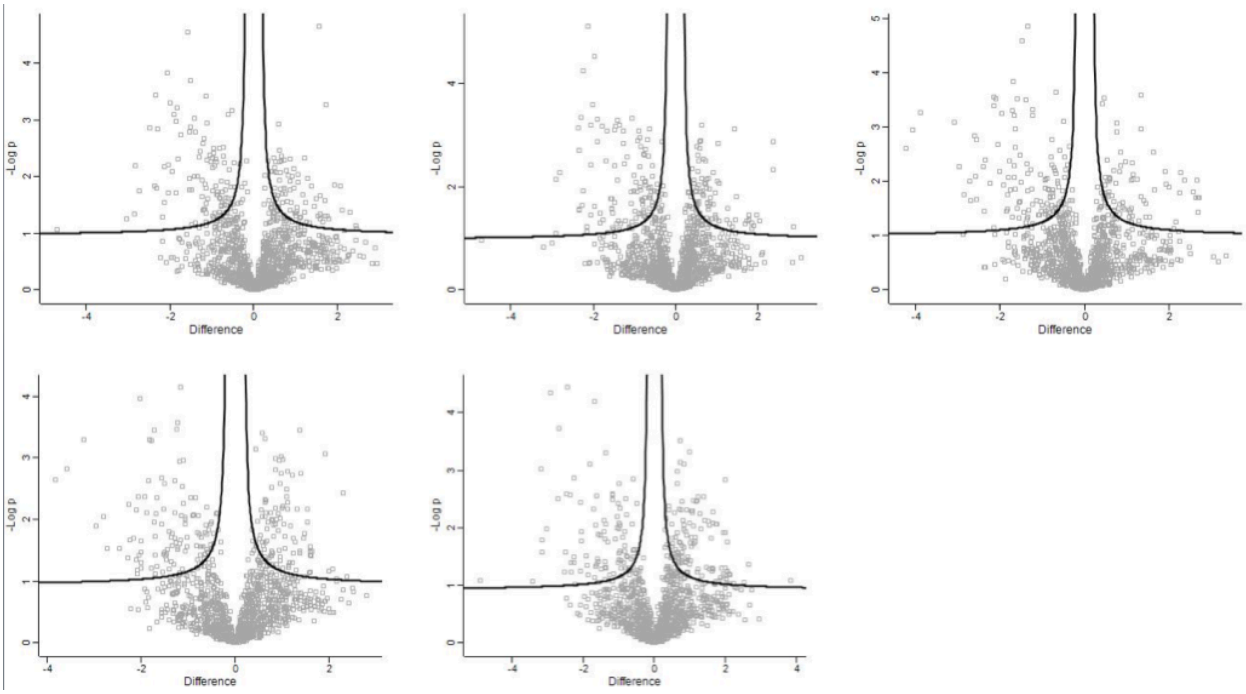

Supplementary figure 3: Volcano plots showing the significant phosphopeptides from the 5 paired t-tests performed on the HT29 cell samples. Each of the inhibitor treatments were paired with the control and a t-test was performed with a permutation-based FDR of <0.2. From top left to bottom right; dabrafenib, GDC0941, CX-4945, Dab+GDC and Dab+CX.

Supplementary table 1: Over-represented annotation categories from the phosphopeptides that were down-regulated in response to BRAF inhibition in HT29 cells

Category column	Category value	Total size	Selection size	Category size	Intersection size	Enrichment factor	Benj. Hoch. FDR
Motifs	JNK kinase substrate motif	620	72	1	1	8.61	0.18
Motifs	CDK4 kinase substrate motif	620	72	3	2	5.74	0.07
Motifs	p70 Ribosomal S6 kinase substrate motif	620	72	10	5	4.31	0.01
Multiplicity	___3	620	72	21	10	4.10	0.00
Motifs	Pim1 kinase substrate sequence	620	72	14	6	3.69	0.01
Motifs	HMGCoA Reductase kinase substrate motif	620	72	8	3	3.23	0.08
Motifs	Aurora-A kinase substrate motif	620	72	9	3	2.87	0.10
Motifs	ZIP kinase substrate motif	620	72	32	10	2.69	0.01
Motifs	AMP-activated protein kinase substrate motif	620	72	30	9	2.58	0.01
Motifs	GSK3 kinase substrate motif	620	72	114	32	2.42	0.00
Motifs	Plk1 PBD domain binding motif	620	72	88	24	2.35	0.00
Motifs	MDC1 BRCT domain binding motif	620	72	88	24	2.35	0.00
Multiplicity	___2	620	72	200	54	2.33	0.00
Motifs	Pyruvate dehydrogenase kinase substrate motif	620	72	90	24	2.30	0.00
Motifs	PAK2 kinase substrate motif	620	72	30	8	2.30	0.03
Motifs	AMP-activated protein kinase 2 substrate motif	620	72	15	4	2.30	0.10
Motifs	Phosphorylase kinase substrate motif	620	72	41	10	2.10	0.03
Motifs	MAPKAPK1 kinase substrate motif	620	72	65	15	1.98	0.00
Motifs	GSK3, ERK1, ERK2, CDK5 kinase substrate motif	620	72	13	3	1.98	0.00
Motifs	Akt kinase	620	72	68	15	1.89	0.00

Supplementary table 2: Over-represented annotation categories from the phosphopeptides that were down-regulated in response to PI3K inhibition in HT29 cells

Category column	Category value	Total size	Selection size	Category size	Intersection size	Enrichment factor	q-value
Motifs	HMGCoA Reductase kinase substrate motif	671	74	7	3	3.89	0.07
Motifs	NIMA kinase substrate motif	671	74	5	2	3.63	0.18
Multiplicity	___3	671	74	32	12	3.40	0.00
Motifs	AMP-activated protein kinase substrate motif	671	74	29	10	3.13	0.01
Motifs	p70 Ribosomal S6 kinase substrate motif	671	74	13	4	2.79	0.08
Motifs	GSK3 kinase substrate motif	671	74	126	29	2.09	0.00
Multiplicity	___2	671	74	222	48	1.96	0.00
Motifs	ZIP kinase substrate motif	671	74	44	9	1.85	0.07
Motifs	DNA dependent Protein kinase substrate motif	671	74	120	24	1.81	0.01
Motifs	Chk1 kinase substrate motif	671	74	63	12	1.73	0.06
Motifs	Plk1 PBD domain binding motif	671	74	98	18	1.67	0.04
Motifs	MDC1 BRCT domain binding motif	671	74	98	18	1.67	0.05
Motifs	Pyruvate dehydrogenase kinase substrate motif	671	74	93	17	1.66	0.05
Motifs	Casein kinase I substrate motif	671	74	163	29	1.61	0.02
Amino acid	T	671	74	92	16	1.58	0.05
Motifs	CDK kinase substrate motif	671	74	119	20	1.52	0.06
Motifs	MAPKAPK2 kinase substrate motif	671	74	157	26	1.50	0.04

Supplementary table 3: Over-represented annotation categories from the phosphopeptides that were down-regulated in response to protein kinase CK2 inhibition in HT29 cells

Category column	Category value	Total size	Selection size	Category size	Intersection size	Enrichment factor	q-value
Charge	5	624	56	1	1	11.14	0.12
Motifs	GSK3, Erk1, Erk2 and CDK5 kinase motif	624	56	17	4	2.62	0.17
Multiplicity	___3	624	56	30	7	2.60	0.01
Motifs	GSK3 kinase substrate motif	624	56	110	20	2.03	0.01
Multiplicity	___2	624	56	199	36	2.02	0.00
Amino acid	T	624	56	89	16	2.00	0.01
Motifs	Plk1 PBD domain binding motif	624	56	91	16	1.96	0.03
Motifs	MDC1 BRCT domain binding motif	624	56	91	16	1.96	0.04
Motifs	BARD1 BRCT domain binding motif	624	56	64	11	1.92	0.08
Motifs	Pyruvate dehydrogenase kinase substrate motif	624	56	93	15	1.80	0.06
Motifs	Phosphorylase kinase substrate motif	624	56	44	7	1.77	0.20
Motifs	MAPKAPK2 kinase substrate motif	624	56	144	21	1.63	0.04
Motifs	CDK kinase substrate motif	624	56	110	15	1.52	0.13

Supplementary table 4: Over-represented annotation categories from the phosphopeptides that were down-regulated in response to combined BRAF/PI3K inhibition in HT29 cells

Category column	Category value	Total size	Selection size	Category size	Intersection size	Enrichment factor	q-value
Motifs	RAF1 kinase substrate motif	610	89	5	3	4.11	0.10
Multiplicity	___3	610	89	28	12	2.94	0.00
Multiplicity	___2	610	89	184	52	1.94	0.00
Motifs	BARD1 BRCT domain binding motif	610	89	61	16	1.80	0.05
Motifs	Casein kinase I substrate motif	610	89	140	35	1.71	0.00
Amino acid	T	610	89	79	19	1.65	0.02
Motifs	b-Adrenergic Receptor kinase substrate motif	610	89	162	38	1.61	0.00
GOMF name	nucleic acid binding	610	89	197	46	1.60	0.02
Motifs	DNA dependent Protein kinase substrate motif	610	89	113	26	1.58	0.04
Motifs	GSK3 kinase substrate motif	610	89	114	26	1.56	0.04
Motifs	Pyruvate dehydrogenase kinase substrate motif	610	89	84	19	1.55	0.10

Supplementary table 5: Over-represented annotation categories from the phosphopeptides that were up-regulated in response to combined BRAF/protein kinase CK2 inhibition in HT29 cells

Category column	Category value	Total size	Selection size	Category size	Intersection size	Enrichment factor	q-value
Motifs	JNK kinase substrate motif	612	64	1	1	9.56	0.16
Motifs	PKR kinase substrate motif	612	64	3	2	6.38	0.07
Motifs	Aurora-A kinase substrate motif	612	64	11	5	4.35	0.01
Motifs	HMGCoA Reductase kinase substrate motif	612	64	10	4	3.83	0.04
Motifs	Pim1 kinase substrate sequence	612	64	20	7	3.35	0.01
Motifs	PKC epsilon kinase substrate motif	612	64	61	20	3.14	0.00
Motifs	PAK2 kinase substrate motif	612	64	40	13	3.11	0.00
Motifs	AMP-activated protein kinase substrate motif	612	64	30	9	2.87	0.01
Motifs	CLK1 kinase substrate motif	612	64	17	5	2.81	0.05
Motifs	p70 Ribosomal S6 kinase substrate motif	612	64	14	4	2.73	0.09
Motifs	AMP-activated protein kinase 2 substrate motif	612	64	18	5	2.66	0.06
Multiplicity	___3	612	64	28	7	2.39	0.01
Motifs	Phosphorylase kinase substrate motif	612	64	45	11	2.34	0.01
Motifs	MAPKAPK1 kinase substrate motif	612	64	79	19	2.30	0.00
Motifs	ATM kinase substrate motif	612	64	21	5	2.28	0.09
Motifs	Calmodulin-dependent protein kinase I substrate motif	612	64	22	5	2.17	0.10
Motifs	Chk1 kinase substrate motif	612	64	62	14	2.16	0.01
Motifs	Calmodulin-dependent protein kinase IV substrate motif	612	64	58	13	2.14	0.01
Motifs	Akt kinase substrate motif	612	64	76	17	2.14	0.00
Motifs	GSK3, Erk1, Erk2 and CDK5 kinase motif	612	64	18	4	2.13	0.14
Motifs	ZIP kinase substrate motif	612	64	43	9	2.00	0.05
Motifs	GSK3 kinase substrate motif	612	64	119	23	1.85	0.00
Motifs	MAPKAPK2 kinase substrate motif	612	64	148	28	1.81	0.00
Multiplicity	___2	612	64	197	36	1.75	0.00
Motifs	14-3-3 domain binding motif	612	64	188	34	1.73	0.00
Motifs	Calmodulin-dependent protein kinase II substrate motif	612	64	208	37	1.70	0.00
Motifs	Pyruvate dehydrogenase kinase substrate motif	612	64	75	12	1.53	0.09
Motifs	PKA kinase substrate motif	612	64	356	56	1.50	0.00

Supplementary table 6: Over-represented annotation categories from the phosphopeptides that were down-regulated in response to combined BRAF/protein kinase CK2 inhibition in HT29 cells

Category column	Category value	Total size	Selection size	Category size	Intersection size	Enrichment factor	q-value
Charge	5	626	85	1	1	7.36	0.14
Motifs	Pyruvate dehydrogenase kinase substrate motif	626	85	81	21	1.91	0.01
Motifs	Plk1 PBD domain binding motif	626	85	85	20	1.73	0.03
Motifs	MDC1 BRCT domain binding motif	626	85	85	20	1.73	0.03
Motifs	Casein kinase I substrate motif	626	85	145	33	1.68	0.01
Charge	4	626	85	22	5	1.67	0.14
Multiplicity	___3	626	85	27	6	1.64	0.13
Motifs	MAPKAPK2 kinase substrate motif	626	85	148	32	1.59	0.01
Multiplicity	___2	626	85	209	45	1.59	0.00
Amino acid	T	626	85	89	19	1.57	0.03
Motifs	b-Adrenergic Receptor kinase substrate motif	626	85	171	35	1.51	0.01
Motifs	Casein kinase II substrate motif	626	85	459	75	1.20	0.01
Charge	3	626	85	290	46	1.17	0.06
Motifs	G protein-coupled receptor kinase 1 substrate motif	626	85	336	53	1.16	0.16
Charge	2	626	85	419	64	1.12	0.08
Multiplicity	___1	626	85	520	72	1.02	0.12

Supplementary table 7: Over-represented annotation categories from the phosphopeptides that were up-regulated in response to BRAF inhibition in Colo205 cells

Category column	Category value	Total size	Selection size	Category size	Intersection size	Enrichment factor	q-value
Motifs	ERK1, ERK2, SAPK, CDK5 and GSK3 kinase substrate motif	403	46	2	2	8.76	0.09
Motifs	Pim1 kinase substrate sequence	403	46	12	5	3.65	0.05
Motifs	ZIP kinase substrate motif	403	46	27	9	2.92	0.02
Motifs	Chk1 kinase substrate motif	403	46	45	15	2.92	0.00
Multiplicity	___3	403	46	7	2	2.50	0.15
Motifs	Calmodulin-dependent protein kinase IV substrate motif	403	46	43	12	2.44	0.02
Motifs	AMP-activated protein kinase substrate motif	403	46	34	7	1.80	0.19
Motifs	PKC epsilon kinase substrate motif	403	46	39	8	1.80	0.16
Motifs	CDK1,2,4,6 kinase substrate motif	403	46	52	10	1.68	0.15
Motifs	Cdc2 kinase substrate motif	403	46	52	10	1.68	0.16
Motifs	Calmodulin-dependent protein kinase II substrate motif	403	46	151	28	1.62	0.01
Motifs	Pyruvate dehydrogenase kinase substrate motif	403	46	51	9	1.55	0.19
Amino acid	T	403	46	58	10	1.51	0.17